Thermoporomechanics of creeping landslides: The 1963 Vaiont slide, northern Italy

Emmanuil Veveakis,[1] Ioannis Vardoulakis,[1] and Giulio Di Toro[2,3]

Received 29 September 2006; revised 27 February 2007; accepted 25 April 2007; published 25 September 2007.

[1] The catastrophic Vaiont landslide (Southern Alps, Italy) of 9 October 1963 moved 2.7×10^8 m^3 of rock that collapsed in an artificial lake, causing a giant wave that killed 1917 people. The landslide was preceded by 2–3 years of creep that ended with the final collapse of the rock mass slipping at about 30 m s^{-1}. Assuming that creep was localized in a clay-rich water-saturated layer, in this study we propose shear heating as the primary mechanism for the long-term phase of accelerating creep. We study only the creeping phase of the slide, and we model this phase using a rigid block moving over a thin zone of high shear strain rates. Introducing a thermal softening and velocity strengthening law for the basal material, we reformulate the governing equations of a water-saturated porous material, obtaining an estimate for the collapse time of the slide. Our model is calibrated upon real velocity measurements from the Vaiont landslide and provides an estimation of the critical time of failure up to 169 days before the collapse. We also show that the slide became critical ~21 days before the collapse, when shear heating started localizing in the clay-rich layer, inducing a tendency for slip localization and thermal runaway instability in a plane. The total loss of strength in the slipping zone during the last minutes prior to the slide is explained by the onset of thermal pressurization, triggered by the temperature rise within the clay-rich layer.

Citation: Veveakis, E., I. Vardoulakis, and G. Di Toro (2007), Thermoporomechanics of creeping landslides: The 1963 Vaiont slide, northern Italy, *J. Geophys. Res.*, *112*, F03026, doi:10.1029/2006JF000702.

1. Introduction

[2] Large catastrophic slope failures are probably preceded by weeks to decades or more of accelerating creep [*Voight*, 1978]. However, such precursory phenomena often pass unnoticed, given their small magnitude or the absence of monitoring instrumentation [*Kilburn and Petley*, 2003]. An exception is the Vaiont slide of October 9, 1963 in northern Italy, as economic interests related to the exploitation of an artificial water reservoir led to the installation of a dense network of instruments (benchmarks, a seismometer, piezometers) to monitor the creeping slope [*Carloni and Mazzanti*, 1964]. Slope monitoring revealed that the slide was preceded by 2–3 years of accelerating creep that concluded with 2.7×10^8 m^3 of rock sliding at ~30 m s^{-1} [*Selli and Trevisan*, 1964; *Carloni and Mazzanti*, 1964; *Ciabatti*, 1964; *Müller*, 1964; *Semenza*, 1965; *Anderson*, 1980; *Hendron and Patton*, 1985]. Several studies focused on the mechanics of the final collapse of the slide (i.e., the last seconds when the slide acceleration was significant) in order to explain the large slip velocities achieved [*Anderson*, 1980; *Voight and Faust*, 1982; *Hendron and Patton*, 1985; *Vardoulakis*, 2002a]. *Müller* [1964, p. 148] in his report about the slide claimed that during the final collapse the strength in the slipping zone reduced spontaneously, and all the potential energy of the sliding mass was converted in kinetic energy. He summarizes his impressions as follows:

> ...the interior kinematic nature of the mobile mass, after having reached a certain limit velocity at the start of the rock slide, must have been a kind of thixotropy. This would explain why the mass appears to have slid down with an unprecedented velocity which exceeded all expectations. Only a spontaneous decrease in the interior resistance to movement would allow one to explain the fact that practically the entire potential energy of the slide mass was transformed without internal absorption of energy into kinetic energy. Such a behaviour of the sliding mass was beyond any possible expectation; nobody predicted it and the author believes that such a behavior was in no way predictable....

[3] *Habib* [1967, 1975] on the basis of the observations of *Müller* [1964] proposed that the high slip velocity achieved by the Vaiont landslide was due to the conversion of mechanical energy into heat during frictional sliding that should lead to the "vaporization" of pore water that produced in turn a cushion of zero friction. Temperature increase in the slipping zone may also have led to pressurization of pore water with the same effect [*Anderson*, 1980; *Voight and Faust*, 1982; *Vardoulakis*, 2000, 2002a]. Total loss of strength by thermal pressurization has also been claimed for the Jiufengershan rock and soil avalanche

[1] Department of Mechanics, Faculty of Applied Mathematics and Physics, National Technical University of Athens, Athens, Greece.
[2] Dipartimento di Geoscienze, Università di Padova, Padua, Italy.
[3] Istituto di Geoscienze e Georisorse, Unità operativa di Padova, Consiglio Nazionale delle Ricerche, Padua, Italy.

0148-0227/07/2006JF000702

triggered by the Chi-Chi (Taiwan) 1999 earthquake [*Chang et al.*, 2005a, 2005b]. *Sitar et al.* [2005] on the other hand showed that in order to obtain such high slip velocities, the aforementioned reduction of the frictional resistance should have been accompanied by internal disintegration of the slide mass.

[4] All the above theories propose thermal pressurization as the most probable mechanism for the loss of strength in the slipping zone. *Vardoulakis* [2000, 2002a] analyzed the phase of the Vaiont slide when thermal pressurization sets in (the so-called pressurization phase), during which the slide accelerates in short time. The pressurization phase is indeed short and the total displacement achieved during this phase is insignificant and thus the rigid block assumption remains an acceptable approximation [cf. *Sitar et al.*, 2005]. In these studies *Vardoulakis* [2000, 2002a] proposed a one-degree-of-freedom, frictional pendulum model and the hypothesis that frictional heating triggered pressurization of pore water inside a forming shear band. This analysis showed that during the pressurization phase the deformation was localized in a very narrow shear band, whose thickness was of $\sim$1 mm, and that the catastrophic pressurization phase of the Vaiont slide should not have taken more than a few seconds to develop in full.

[5] Although the physical mechanisms that govern the last minutes of the Vaiont slide were explored in some detail, the same claim is not valid for the 2–3 years of "slow" creeping motion that preceded the assumed pressurization phase. Several studies reproduced the velocity history of the slide and explained the deformation mechanisms of the final collapse, but there are still many questions on the mechanism that triggered the pressurization phase. *Helmstetter et al.* [2004] and *Sornette et al.* [2004] analyzed the landslides of Vaiont and La Clapière (southeastern French Alps) using a slider block model and the rate and state friction law by *Dieterich* [1978] and *Ruina* [1983]. They proposed a "velocity law" for the time evolution of slide velocity V, that provides a useful estimate for the "blowup time" or the "lifetime of the slide" t_l,

$$V \approx \frac{U}{t_l - t} \tag{1}$$

where U is a constant. The blowup time t_l is defined as the time at which the slide will collapse. A similar empirical model was proposed earlier by *Voight* [1988] and was used in the case of Vaiont also by *Kilburn and Petley* [2003], *Sornette et al.* [2004] and *Petley et al.* [2005]. In this model, displacement data during an accelerating phase are plotted in the (Λ-t) space, where $\Lambda = 1/V$ is the inverse velocity of the slide and t is the time. In the case of deformation caused by progressive crack growth, the (Λ-t) diagram can be approximated by a linear function providing a forecast for the Vaiont slide up to 60 days before the final collapse. However, when deformation is dominated by sliding on a preexisting slip surface (as is the case for the Vaiont slide according to *Hendron and Patton* [1985]) or is the result of ductile deformation, according to *Kilburn and Petley* [2003] the above approach should not be applied.

[6] In this study we focus on the mechanics of the long creeping phase up until the pressurization phase, where the rigid block assumption remains an acceptable approximation (see section 3.3). Our analysis is based on the working hypothesis that the Vaiont slide during the creeping phase was localized in 0.5 to 17.5 cm thick clay-rich layers, embedded in the limestone [*Hendron and Patton*, 1985]. We propose here a model that accounts for heat production due to friction at the base of the slide, that turns out to be compatible with the hyperbolic velocity law (equation (1)). We relate the creeping motion to a thermally self-driven transient creep process, which is followed by progressive shear heating localization that eventually triggers the catastrophic pressurization phase inside the slipping zone. The model is kept as simple as possible, in order to make the mathematical formulation tractable and to explore the limitations of the shear heating mechanism. For this purpose, we neglect mechanisms that may be important during the evolution of the Vaiont slide in its entirety, such as (1) the evolution of the shear stress due to the water table variations [*Hendron and Patton*, 1985], (2) the flash heating effects that may also reduce the frictional strength of the clay-rich layer [*Rice*, 2006], (3) the complex mechanisms that govern the transition from critical to residual conditions at the onset of the pressurization phase [*Vardoulakis*, 2002a], (4) the possible pore pressure feedbacks due to the contractant or dilatant behavior of the basal shear zone and their relationship to unstable acceleration [*Iverson*, 2005], and (5) the realistic modeling of energy dissipation inside the rock mass at the final stage of a fully developed slide [*Sitar et al.*, 2005].

2. Geology of the Vaiont Slide

[7] The Vaiont landslide of October 9, 1963, has been the subject of numerous geological and geomechanical investigations, for its potential contribution in slope stability analysis and for the social and legal implications of the disaster [*Carloni and Mazzanti*, 1964; *Müller*, 1964; *Selli and Trevisan*, 1964; *Semenza*, 1965]. A detailed study of the geology and mechanics of the slide is given by *Hendron and Patton* [1985, and references therein]; here we summarize the most relevant aspects for our analysis. The landslide moved approximately 2.7×10^8 m^3 of rock from the northern flank of the Mount Toc into an artificial reservoir of about 1.5×10^8 m^3 impounding the east-west trending Vaiont deep gorge. Dam building and water impounding begun in July 1957 and February 1960, respectively. The slide moved a $\sim$120 m thick (on average) compact rock mass over a front of 1850 m for a maximum slip of 450–500 m [*Selli and Trevisan*, 1964] and at a final slip rate of about 25–30 m s^{-1} [*Anderson*, 1980, 1985]. The abrupt debris filling of the reservoir produced a giant wave (4.8×10^7 m^3) that propagated up and down the valley, overflowed the dam and wiped out the village of Longarone, located 2 km westward [*Selli and Trevisan*, 1964].

[8] The landslide occurred on a chair-shaped fold, with the axis plunging 9° to 20° eastward and parallel to the Vaiont Valley. In north/south cross sections, the seat of the monocline is horizontal (though it dips 9° to 20° eastward) and, south of the fold axis (i.e., the Mount Toc flank), the back of the slide dips 25° to 40° north, providing the driving force for the slide (Figure 1a). The landslide occurred on an unstable slope where glacial to historic landslides had occurred [*Semenza*, 1965]. The slide reused a preexisting

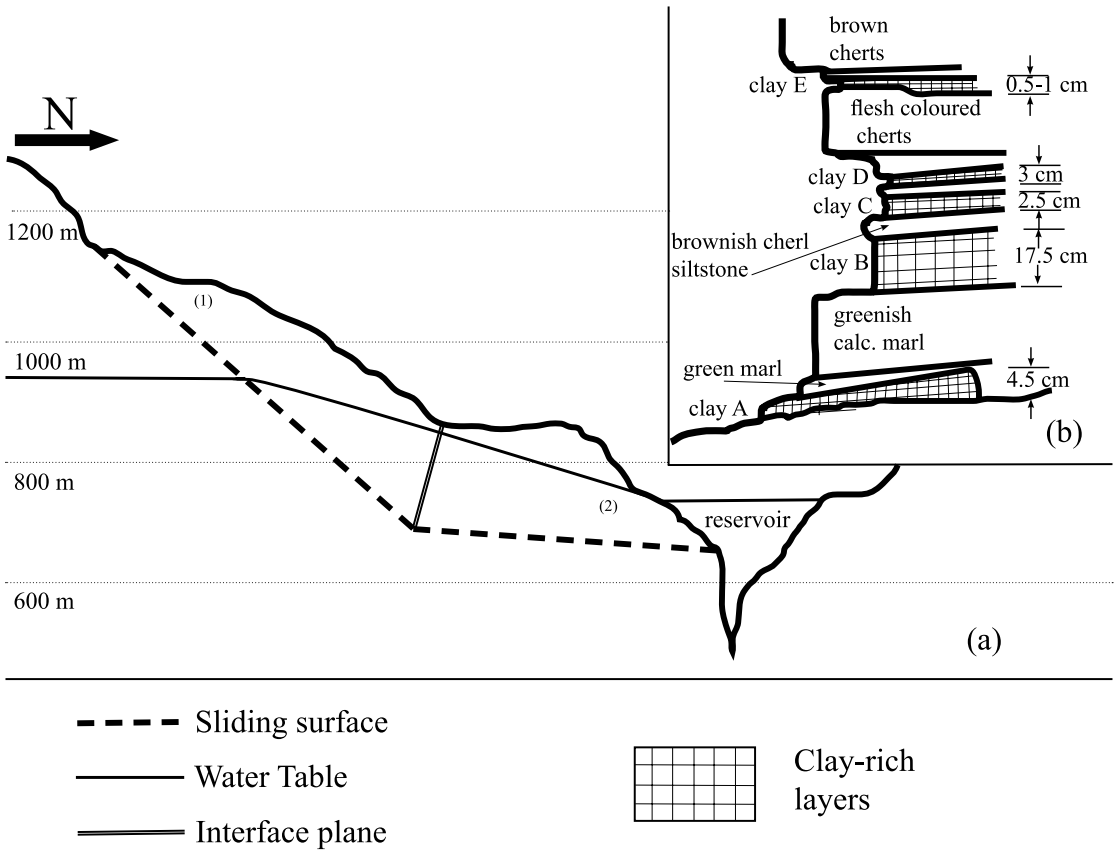

Figure 1. Geology of the Vaiont slide. (a) "Chair" failure mechanism of the Vaiont slide, reconstructed from *Müller-Saltzburg* [1968]. The back of the chair is assumed to dip at 40.5°, while the seat is almost horizontal, dipping at 2.5°. (b) Stratigraphy of the rocks of the Vaiont sliding surface. This sequence is found in outcrops in the Vaiont area at the same stratigraphic position as those at the base of the Vaiont slide. Slip is thought to have been confined in the clay-rich layers. To the right, thickness is given in centimeters. Redrawn from *Hendron and Patton* [1985].

surface of rupture [*Hendron and Patton*, 1985]. This is suggested by the early presence (from October 1960) of deep trenches in the flank of Mount Toc which outlined the southern limit of the October 1963 landslide [*Semenza*, 1965].

[9] The stratigraphy of the slide area includes a succession of limestones and marls [*Carloni and Mazzanti*, 1964; *Semenza*, 1965]. The slide occurred at the top of >0.5 m thick limestone strata, with the failure surface consisting of 0.05–0.3 m thick strata of limestone and marl intercalated by clay rich layers. Slip was confined within 0.5–17.5 cm thick clay-rich layers, which were continuous over large areas of the surface of failure [*Hendron and Patton*, 1985] (Figure 1b). Clay-rich layers were a mixture of 35–80% in clays (Ca-montmorillonite, smectite, illite, vermiculite) by mass and grains of calcite and minor quartz [*Broili*, 1967; *Hendron and Patton*, 1985]. These clays had low shear strengths (friction coefficient of 0.10–0.17), an expanding lattice, and swelling properties in the presence of water.

[10] The landslide was characterized by a long-term phase of accelerating creeping lasting ~2–3 years with ~3 m of slip (0.2 m on 9 October 1963 [see *Müller et al.*, 1964], followed by the catastrophic failure [*Selli and Trevisan*, 1964]. A similar accelerating creeping phase (~1.3 m of creep accommodated in 2–3 months) preceded the slide of November 4 1960 that occurred in the same area, though limited to 7×10^5 m^3 of rock [*Semenza*, 1965]. It is noteworthy that microseismicity from the creeping slope was recorded few weeks before and after the 4 November 1960 slide, from February to December 1962 and, lastly, in July 1963. The catastrophic October 1963 failure was not preceded by microseismicity [*Carloni and Mazzanti*, 1964; *Belloni and Stefani*, 1992].

[11] The October 1963 landslide was the result of the installation and impounding of the artificial reservoir, probably together with the contribution of rainfall/snowmelt. According to *Hendron and Patton* [1985], the plots of cumulative precipitation versus reservoir level for the 30 days prior the slide, resulted in a "failure envelope". This failure envelope yielded the combination of reservoir level versus cumulative precipitation that would have caused the pore pressure rise necessary to overcome the slope strength. Although the idea is intriguing, according to *Kilburn and Petley* [2003] the mechanics of the accelerating creep still remain unclear and call for further research.

3. Modeling a Thermally Driven, Creeping Slide

[12] The problem of a creeping landslide, which is accompanied by heat production due to friction on its base

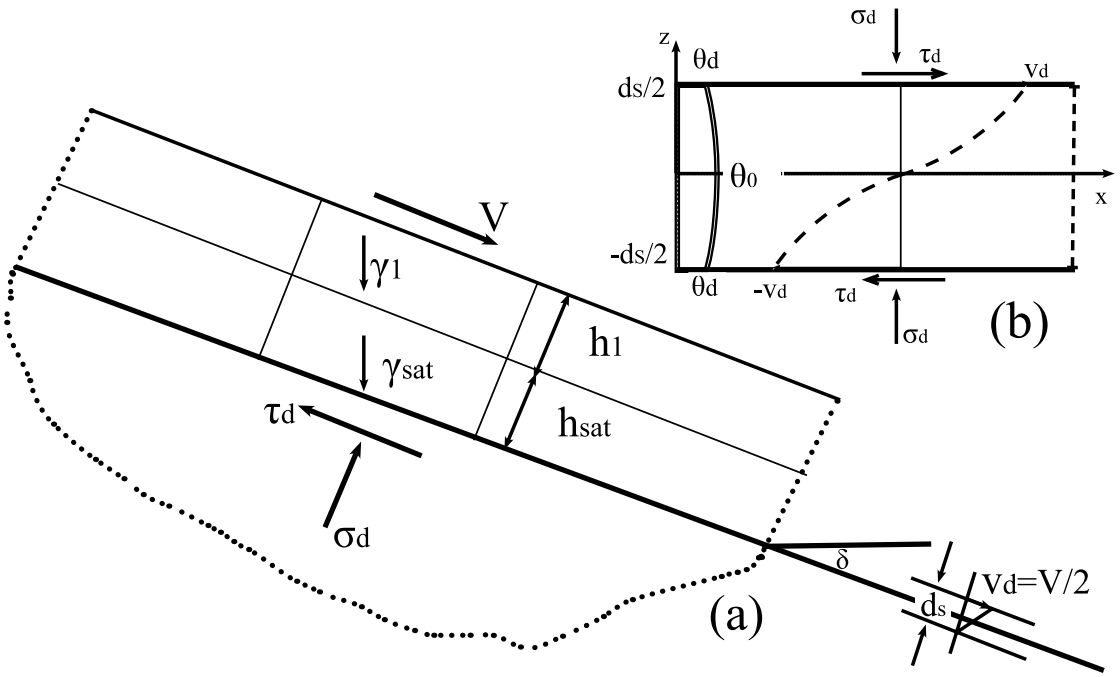

Figure 2. Modeling a thermally driven creeping landslide. (a) Rigid block divided into two domains: the upper, dry material, γ_1, and the lower, saturated material, γ_{sat}. (b) Thin shear zone, on which the block is sliding. The steady state profiles of the temperature (θ) and the velocity (v) fields indicate that the model is based on the concept that in a thermoviscoplastic material, high-velocity gradients counterbalance high temperatures resulting in constant critical state friction coefficient throughout the process [*Vardoulakis*, 2002b].

(hereafter called a thermally driven slide), is approached here by a simple model of a rigid block (the compact rock mass) that slides over a thin shear zone (the clay-rich layer, see Figure 2). For simplicity we assume that all the mechanical fields vary along the ''short'' z axis (Figure 2b), thus establishing a one dimensional model. In this section, we construct the governing equations of the rigid block and of the shear zone and discuss the critical parameters that characterize the model. Inside the block, since it is rigid, the momentum balance dominates; inside the shear zone, since it is in a quasi-static condition with negligible acceleration, mass and energy balances dominate the behavior of the material. The rigid block and the shear zone are coupled at the upper shear zone boundary, which constitutes the common interface between the two structures. It is assumed that at this interface no slip discontinuity is taking place. Thus the velocity field is assumed to be continuous. Similarly, owing to local equilibrium, the normal and shear stresses are continuous across this interface.

3.1. Thermal Pressurization Coefficient

[13] In this section we introduce the pore pressure diffusion equation that describes the drainage within the clay-rich, water-saturated shear zone and we provide an estimate of (1) the pressurization coefficient (i.e., the parameter that couples temperature increase with pore pressure generation) and (2) the critical pressurization temperature (i.e., the temperature at which clays start to dehydrate [*Nova*, 1986]), which determines the onset of the thermal pressurization phase.

[14] We consider the shear zone as a two-phase material made of a solid skeleton and of a fluid. The fluid fills completely the voids and can flow inside the pore space. The total density of a fully saturated medium is

$$\rho = (1-\phi)\rho_S + \phi\rho_W \tag{2}$$

where ϕ is the porosity and ρ_S, ρ_W the density of the solids and of the water (fluid), respectively. Under rapid loading, drainage is governed by the corresponding excess pore water pressure diffusion equation [*Vardoulakis*, 2002c],

$$\frac{\partial \Delta p}{\partial t} = c_V \frac{\partial^2 \Delta p}{\partial z^2} + \lambda_m \frac{\partial \theta}{\partial t} \tag{3}$$

where c_v is the consolidation coefficient, Δp is the excess pore pressure, λ_m is the pressurization coefficient and θ is the temperature. The consolidation coefficient of clays is in general a weakly increasing function of the temperature [*Delage et al.*, 2000]. For simplicity we will assume here that c_v is constant [*Vardoulakis*, 2002a]. According to *Vardoulakis* [2002a] the pressurization coefficient of a clay can be expressed as

$$\lambda_m \approx \frac{-\alpha_c^p}{c} \tag{4}$$

where α_c^p is the plastic thermal expansion coefficient of the soil skeleton, and c is the compressibility coefficient.

[15] The existing data for λ_m in clays are scarce (see *Sulem et al.* [2007] for a comprehensive discussion on λ_m).

Drained triaxial tests on Boom clay, reported by *Sultan* [1997], showed that both λ_m and the critical temperature θ_{cr}, at which thermal pressurization sets in, are functions of the degree of the compaction. In soil mechanics, the compaction of a clay is related to the largest past effective stress, called the preconsolidation stress $\sigma'_c = \sigma_c + p_w$, where σ_c is the normal stress and p_w is the pore water pressure (stresses are taken positive in tension). Clays that are precompacted are called ''overconsolidated'' and the ''overconsolidation'' ratio (OCR = σ'_c/σ' or ratio of the largest past experienced effective normal stress σ'_c over the current effective normal stress during shear) quantifies the degree of precompaction [*Wood*, 1990]. Both λ_m and θ_{cr} can be expressed as functions of OCR: ''over''-consolidated clays have small values for λ_m and high values for θ_{cr} [*Vardoulakis*, 2002a, Figure 11].

[16] Heavily ''overconsolidated'' clays dilate under shear. Large shear displacements tend to erase the memory of a clay on its past compaction history, forcing it to behave like a ''normally'' consolidated clay (i.e., a clay which is sheared at the same effective normal stress as it has been compacted). Back extrapolation of the experimental data reported by *Sultan* [1997] for λ_m and θ_{cr} as functions of the OCR to the value OCR = 1 (i.e., corresponding to ''normally'' consolidated clay), yields $\lambda_m|_{OCR=1} \approx 0.07$ MPa/°C and $\theta_{cr}|_{OCR=1} \approx 36$°C [*Vardoulakis*, 2002a]. This estimate of θ_{cr} is typical for clays, and it is higher than the groundwater temperature (the annual average air temperature in the Vaiont area is 7.9°C [*Besio*, 1992]) at a depth of about 120 m where the sliding surface of the Vaiont slide was located [*Müller-Saltzburg*, 1968].

3.2. Heat Equation in the Shear Zone

[17] The heat equation in the shear zone includes two contrasting effects: heat loss by conduction and heat production by deformation [*Vardoulakis*, 2002c]. The basic assumptions made here are the following:

[18] 1. The two phases (i.e., the solid and the aqueous) are always in thermal equilibrium. This allows us to define a unique temperature field, $\theta(z, t)$, for both phases.

[19] 2. The heat flux vector obeys Fourier's law for thermally isotropic media, $Q = -jk_m \frac{\partial\theta}{\partial z}$, where $j = 4.2$ J/kcal is the mechanical equivalent of heat [*Planck*, 1945], and $k_m = (1 - \phi)k_s + \phi k_w$ is the Fourier coefficient of the mixture, with k_s and k_w the thermal conductivity of the solid minerals and of water, respectively.

[20] With the above assumptions the balance law for local entropy production yields the following heat diffusion equation [*Vardoulakis*, 2002a, 2002b]:

$$\frac{\partial\theta}{\partial t} = \kappa_m \frac{\partial^2\theta}{\partial z^2} + \frac{1}{j(\rho C)_m} D_{loc}. \tag{5}$$

In equation (5), D_{loc} is the local dissipation of mechanical work into heat; $\kappa_m = k_m/(\rho C)_m$ is the thermal diffusion coefficient of the mixture, where

$$(\rho C)_m = (1 - \phi)\rho_s C_s + \phi\rho_w C_w \tag{6}$$

is the specific heat of the mixture and C_s, and C_w are the specific heat of the solid minerals and of the water, respectively.

[21] We notice here that the rate of deformation tensor of the solid phase, D_{ij}, is split into an elastic and a viscoplastic part, $D_{ij} = D^e_{ij} + D^{vp}_{ij}$. By neglecting the dissipation in the fluid phase and by assuming that the elastic deformation rate is small if compared to the plastic one, we conclude that $D_{ij} \approx D^{vp}_{ij}$. A basic assumption made here is that the local dissipation of the mixture is expressed as

$$D_{loc} = \sigma'_{ij} D_{ij} \tag{7}$$

i.e., it is assumed that the rate of viscoplastic work is totally converted into heat. We notice however that the classical experiments of *Taylor and Quinney* [1931] on metals revealed that about 20–90% of the input energy is dissipated in heat. This observation resulted in the so-called Taylor heat conduction equation of thermoplasticity. Accordingly the source term, equation (7), was modified by introducing a correction factor β accounting for the efficiency of the system to convert inelastic work to heat,

$$D_{loc} = \beta\sigma'_{ij} D^{vp}_{ij}, \quad 0 < \beta < 1. \tag{8}$$

Rosakis et al. [2000] proposed a general internal-variable theory in order to explain, within a thermodynamic framework, the validity of such a correction to the heat source term and pointed out that indeed this correction factor β is a function of state and can vary in a wide range.

[22] For water-saturated, rapidly sheared clays, there are no experimental data as is the case for metals given by *Taylor and Quinney* [1931]. However, by using equation (8) instead of equation (7) in the heat diffusion equation (5), the correction factor β would be included in the specific heat term of the mixture, $(\rho C')_m = \frac{(\rho C)_m}{\beta}$. *Picard* [1994] determined for water-saturated clays $j(\rho C)_m = 2.85$ MPa/°C. By assuming $\beta \approx 1$, the back analysis performed in Appendix D yielded an estimate for the slipping zone thickness of 16.1 cm, which is in the range of thicknesses (0.5–17.5 cm) of the clay-rich layers from the Vaiont area. Thus we will assume here that, during the long-term creep phase of the slide, all inelastic work in the sheared clay-rich layers is converted into heat.

3.3. Momentum Balance of the Sliding Body

[23] *Sitar et al.* [2005] performed a multibody analysis of the Vaiont slide. They concluded that the Vaiont landslide initially slid as a relatively coherent block on a slipping plane at or very near residual friction before the onset of catastrophic failure. As failure progressed, internal strain in the slide was accommodated by disintegration of the slide mass. The necessity of abandoning the rigid-body assumption for correctly reproducing the final stages of a catastrophic landslide was also acknowledged in *Vardoulakis* [2002a]. It follows that the rigid body model for the sliding rock mass is valid only for the initial phase of the slide motion, i.e., (1) during the prolonged slow creeping phase, where dynamic effects were inappreciable, and (2) until the initial stage of the catastrophic pressurization phase.

[24] In the Vaiont area, clay-rich layers are interbedded with limestone/marl strata (Figure 1); the surface of the strata is sometimes irregular. Although possible, it does not seem very probable that the accelerating creep occurred

Table 1. Properties of the "Chair" Failure Mechanism of Figure 1a

Block	Failure Plane	Length L, m	Dip Angle ϑ, deg	Mean Overburden h, m	Normal Effective Stress $\sigma'_{d,0}$, MPa	Shear Stress $\tau_{d,0}$, MPa
1	"back"	819.9	40.9	113.8	0.92	0.41
2	"seat"	553.5	2.5	128.6	3.48	1.46
2	interface plane	196.5	119.7	–	4.90	2.01

within a single clay-rich layer that eventually failed catastrophically on 9 October 1963. First, the presence of some asperities may impede the smooth and continuous sliding along the entire slip surface. Second, creep may have been partitioned within several clay-rich layers over the large area ($\sim$2 km^2) of the sliding surface. Slip may have jumped from a clay-rich layer to a nearby one, while the limestone/marl in between could have failed under tension. However, the bulk effect of this process, by linking different slipping surfaces, could have been the formation of a principal, clay-rich, sliding surface during the accelerating creep phase.

[25] *Vardoulakis* [2002a] approximated the initial failure mechanism of the Vaiont slide with a rigid body sliding along a circular slip surface. The modified Taylor friction circle analysis provided a friction angle of the clay at incipient failure, $\varphi_F = 22.3°$, and a mean normal effective stress of about $\bar{\sigma}'_{d,0} = 2.4$ MPa, where the subscript "d,0" denotes the initial value of a quantity at the discontinuity plane, which is the interface between the sliding rigid block and the deforming shear layer.

[26] In order to account for some degree for internal breakage of the slide even at an early stage of its history, we performed here a limit analysis of the "chair" failure mechanism of the Vaiont slide, as shown in Figure 1a. In this mechanism, the reservoir elevation is set at 710 m, which is the maximum value for the period between May 1963 (650 m) and October 1963 (710 m). The phreatic surface (water table) is approximated here by using in a piecewise manner the Dupuit-Forchheimer "parabola,"

$$z = \sqrt{c_1 x + c_2} \tag{9}$$

which is sketched in Figure 1a. The two "rigid blocks," 1 and 2, are separated by a plane (the interface plane). Notice that the placement of this plane was also motivated by the reported saddle-shaped region of the slide surface. Assuming a friction angle of the clay at incipient failure, $\varphi_F = 22.3°$ as given by *Vardoulakis* [2002a], we obtain the mean values listed in Table 1 for (1) the normal effective stress, (2) the shear stress acting on the slip planes and (3) the overburden height. For use in the single-block mechanism, weighted average values are computed as follows:

$$\begin{aligned} \bar{\sigma}'_{d,0} &= \frac{1}{h^{(1)} + h^{(2)}} \left(h^{(1)} \sigma'^{(1)}_d + h^{(2)} \sigma'^{(2)}_d \right) = 2.28\,\text{MPa} \\ \bar{\tau}_{d,0} &= \frac{1}{h^{(1)} + h^{(2)}} \left(h^{(1)} \tau^{(1)}_d + h^{(2)} \tau^{(2)}_d \right) = 0.97\,\text{MPa} \end{aligned} \tag{10}$$

Notice that in the pertinent literature the value for the mean basal shear stress $\bar{\tau}_{d,0}$ varies between 0.5 MPa and 2 MPa [*Müller-Saltzburg*, 1968].

[27] In general we assume that the basal shear stress is a function of the effective stress at the interface and of a locally mobilized friction coefficient,

$$\bar{\tau}_d = \bar{\sigma}'_d \mu_d \tag{11}$$

The above mentioned initial values of the shear stress $\bar{\tau}_{d,0}$, the mean normal stress $\bar{\sigma}'_{d,0}$ and the mobilized friction angle at incipient plastic failure φ_F yield a restriction for the equilibrium friction coefficient,

$$\mu_{d,eq} = \frac{\bar{\tau}_{d,0}}{\bar{\sigma}'_{d,0}} = \tan(\varphi_F). \tag{12}$$

Thus from equation (12) and equation (10) we get here also that $\mu_{d,eq} \approx \tan(22.3°)$.

[28] Assuming a single-block mechanism, we have to adjust the dip angle δ of the equivalent single planar surface. The dip angle of the hypothetical surface has to be between the dip angle of the seat and of the back of the aforementioned chair mechanism. The dynamic frictional pendulum analysis indicated that during the final phase of the Vaiont slide motion (when the pressurization phase was fully developed), the maximum acceleration of the slide was $\sim$0.26 g, where g = 9.81 m/s^2 is the acceleration of gravity [*Vardoulakis*, 2002a]. To reach these accelerations with an equivalent planar slip surface, the dip angle of the slip plane is set here as $\delta \approx 15.2°$ (Figure 2), yielding

$$g' = g \sin\delta \approx 2.6\ \text{m/s}^2. \tag{13}$$

[29] Under the above assumptions the dynamic equation for the sliding block yields

$$\tau_d = \tau_{stat} \left(1 - \frac{1}{g'} \frac{dV}{dt} \right), \quad \tau_{stat} = \bar{\tau}_{d,0} \tag{14}$$

where V is the velocity of the sliding block. We can use equation (14) and the data for the velocity of the Vaiont slide, provided by *Müller* [1964], to conclude that the (mean) basal shear stress retains its equilibrium value ($\tau_d \approx \bar{\tau}_{d,0}$) until the very last minutes prior to the catastrophe, when a severe reduction of the basal shear stress is calculated according to equation (14) (Figure 3).

3.4. Thermal Softening and Heat Dissipation Inside the Shear Zone

[30] Viscoplastic flow is a temperature-dependent, exothermal process. This means that when stress is applied, the work done by the resultant flow can increase the rate of heat generation [*Gruntfest*, 1963]. In this manner a regenerative feedback can be developed. When this feedback forces the material to reach a critical point where the effect of velocity strengthening fails to counterbalance the effect of temperature softening, thermal runaway occurs. In the following sections the phenomenon of thermal runaway is studied in relation to the catastrophic Vaiont slide.

[31] As the slide acceleration is negligible until the very last minutes of the slide history, we neglect inertia inside the shear zone. It follows from the momentum balance equation

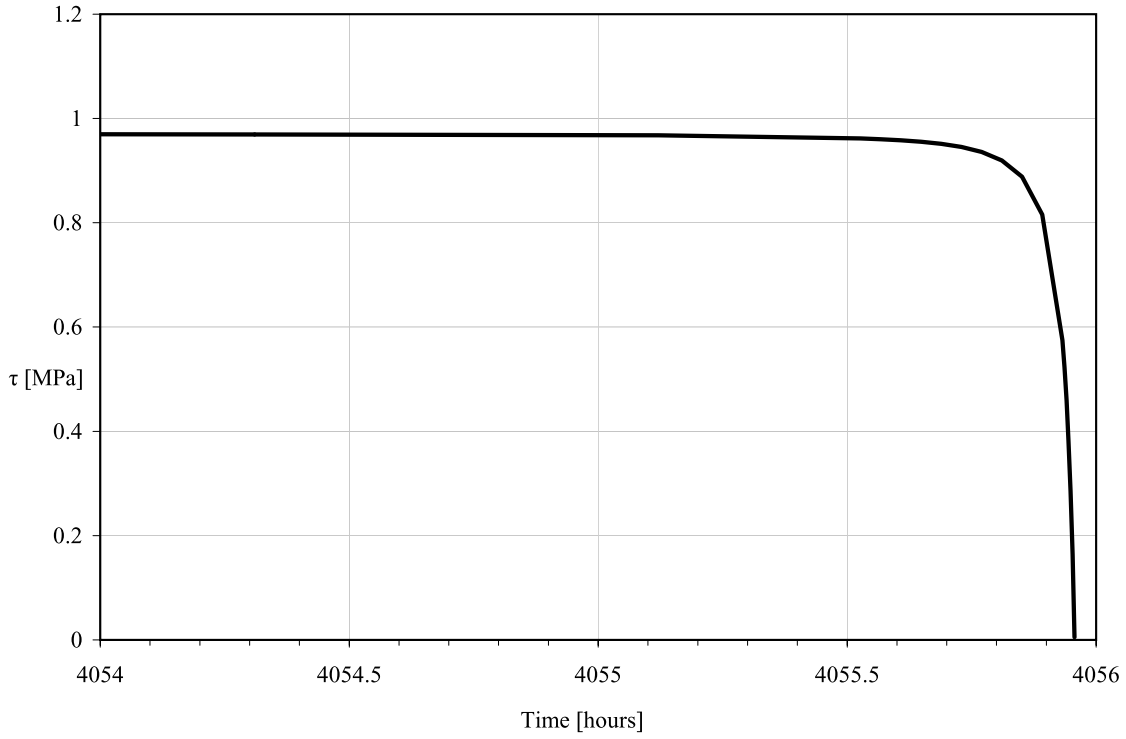

Figure 3. Evolution of the shear stress in the sliding surface during 9 October 1963 (the slide took place on 9 October 1963 at 2239 UT after 169 days of accelerating creep). The reduction in the shear stress is computed from the observed slide velocity [*Müller*, 1964] according to equation (12). The velocity data reveal that significant reduction of the shear stress from its quasi-static value must have taken place during the very last minutes of the slide motion prior to the catastrophe.

that shear stress is practically constant across the shear zone:

$$\frac{\partial \tau}{\partial z} = 0 \Rightarrow \tau = \tau_d = \text{const.} \tag{15}$$

Since during the creeping phase the computed mean shear stress at the discontinuity plane is constant, we assume in addition that the shear zone material is at, or nearly at, a 'critical state', thus deforming under constant volume. In soil mechanics terminology, the critical state is a quasi-stationary state, where the voids ratio of the soil remains constant during shear under constant effective stress [*Wood*, 1990]. At the critical state, mass balance together with Darcy's law result into a constant pore pressure profile across the shear zone. This means that no fluid flow can be sustained across the shear zone and the only remaining dependent variables are the temperature and the velocity of the mixture in the direction of the long axis of the shear zone [*Vardoulakis*, 2002b].

[32] According to equation (7), the rate of mechanical work dissipated in heat is given here by the work of the shear stress on the rate of shear deformation

$$D_{loc} = \sigma_{xz} D_{xz} + \sigma_{zx} D_{zx} \approx \tau_d \frac{\partial v}{\partial z} = \tau_d \dot{\gamma} \tag{16}$$

since $\dot{\gamma} = \partial v/\partial z$. As already mentioned, the shear stress is given formally by a friction law that must be evaluated at the interface between the rigid block and the shear zone. In this law the friction coefficient $\mu_d = \mu_{cs}$ will be identified with the so-called Coulomb friction coefficient at critical state. The μ_{cs} is for some clays an increasing and for others a decreasing function of temperature [*Hicher*, 1974; *Laloui*, 2001, 2005; *Laloui and Cekerevac*, 2003]. Here we will assume that the critical friction angle decreases with increasing temperature (i.e., friction thermal softening [*Vardoulakis*, 2002b]).

[33] In this study, thermal softening is combined with velocity strengthening (the latter is typical for clays [see *Scholz*, 2002]), as the two counterbalancing mechanisms govern the critical state frictional behavior of the clay. Accordingly μ_{cs} is defined by a velocity strengthening power law and a thermal softening exponential law:

$$\mu_{cs} = \mu_{ref} \cdot \left(\frac{\dot{\gamma}}{\dot{\gamma}_{ref}} \right)^N e^{-M(\theta - \theta_1)} \tag{17}$$

where N and M are the frictional rate-sensitivity and the frictional thermal-sensitivity parameters, respectively, and μ_{ref}, $\dot{\gamma}_{ref}$ are reference quantities for the friction coefficient and the strain rate at the reference temperature θ_1. Strain rate friction hardening is viewed here as the necessary counterbalancing effect to thermal softening. At steady state, these two effects have to be in balance, resulting to constant shear stress across the shear zone [see *Vardoulakis*, 2002b, Figure 2b].

[34] From equation (17), the shear stress is given by a nonlinear viscosity law

$$\tau = \sigma_0' \mu_{\mathrm{ref}} \cdot \left(\frac{\dot{\gamma}}{\dot{\gamma}_{\mathrm{ref}}}\right)^{\mathrm{N}} \cdot \mathrm{e}^{-\mathrm{M}(\theta-\theta_1)}. \tag{18}$$

In the case of the Vaiont slide we assume (see Appendix A), N = 0.01, M = 0.0093°C^{-1} and θ_1 = 22°C [*Vardoulakis*, 2002b].

[35] During the creeping phase, the shear stress and the normal effective stress are constant across the shear zone: $\tau = \bar{\tau}_{\mathrm{d},0}$. From equation (18) the shear strain rate is

$$\dot{\gamma} = \dot{\gamma}_0 \mathrm{e}^{\mathrm{m}(\theta-\theta_1)} \tag{19}$$

where

$$\dot{\gamma}_0 = \dot{\gamma}_{\mathrm{ref}} \left(\frac{\bar{\tau}_{\mathrm{d},0}}{\sigma_0' \mu_{\mathrm{ref}}}\right)^{1/\mathrm{N}} \quad \text{and} \quad \mathrm{m} = \frac{\mathrm{M}}{\mathrm{N}}. \tag{20}$$

Thus equation (17) yields a constant critical state friction coefficient,

$$\mu = \mu_0 \left(\frac{\dot{\gamma}}{\dot{\gamma}_0}\right)^{\mathrm{N}} \mathrm{e}^{-\mathrm{M}(\theta-\theta_1)} = \mu_{\mathrm{cs}} = \text{const.} \tag{21}$$

We conclude that during creep the mobilized friction inside the shear zone has a critical state value ($\mu_{\mathrm{cs}} \approx 0.4$). The friction coefficient achieves its residual value ($\mu_{\mathrm{res}} \approx 0.1 \div 0.2$) when pressurization takes over and large shear displacements and shear velocities dominate the process [*Vardoulakis*, 2002a]. In this setting, the local shear dissipation increases linearly with $\bar{\tau}_{\mathrm{d},0}$ and is an exponential function of the temperature:

$$\mathrm{D}_{\mathrm{loc}} \approx \tau_{\mathrm{d}} \dot{\gamma} = \mathrm{D}_0 \mathrm{e}^{\mathrm{m}(\theta-\theta_1)}, \mathrm{D}_0 = \bar{\tau}_{\mathrm{d},0} \dot{\gamma}_0 \tag{22}$$

3.5. Mathematical Model of Shear Heating and Thermal Feedback

[36] Introducing the following set of dimensionless variables:

$$\mathrm{z}^* = \frac{\mathrm{z}}{(\mathrm{d_S}/2)}, \quad \mathrm{t}^* = \frac{\kappa_{\mathrm{m}}}{(\mathrm{d_S}/2)^2}\mathrm{t}, \quad \theta^* = \mathrm{m}(\theta - \theta_1) \tag{23}$$

and using equation (22), the heat equation, equation (5), becomes

$$\frac{\partial \theta^*}{\partial \mathrm{t}^*} = \frac{\partial^2 \theta^*}{\partial \mathrm{z}^{*2}} + \mathrm{Gr}\, \mathrm{e}^{\theta^*}, \quad \mathrm{z}^* \in [-1, 1], \mathrm{t}^* > 0 \tag{24}$$

where

$$\mathrm{Gr} = \mathrm{m} \frac{\dot{\gamma}_0}{\mathrm{j} k_{\mathrm{m}}} \left(\frac{\mathrm{d_S}}{2}\right)^2 \bar{\tau}_{\mathrm{d},0}. \tag{25}$$

The Gr is the Grunfest number [*Gruntfest*, 1963], a dimensionless number representing the effect of the heat generation due to viscoplastic friction in the clay gouge. In the present setting, if the (boundary) shear stress $\bar{\tau}_{\mathrm{d},0}$ is assumed not to vary significantly with time, the Gruntfest number is constant. In general, the Gruntfest number in equation (24) is a function of space and time. We notice also that even for small Gruntfest numbers, the exponential function in equation (24) has a strong thermal feedback that leads to thermal runaway.

[37] The diffusion equation (equation (24)) has been extensively studied in gasdynamics, and it is classified under the name "solid fuel model" or "Frank-Kamenetsky equation." This equation is important in combustion theory, and it presents a finite time singularity in its solution known as the "blowup time" [*Bressan*, 1992; *Galaktionov and Vazquez*, 1997, 2002; *Galaktionov and Harwin*, 2005]. A linear stability analysis of equation (24) for the considered problem (Appendix B) yields that the steady state solution, when it exists, is unconditionally unstable: any small perturbation of the steady state temperature profile would inevitably lead to a finite time blowup [e.g., *Kaplan*, 1963; *Fujita*, 1969; *Friedman and Giga*, 1987].

4. Vaiont Slide From Creep to Collapse

[38] *Müller* [1964, p. 179] summarized his impressions for the long-term creeping behavior of the Vaiont slide as follows:

> . . .The peak velocities increased progressively during the early days of October. According to the report of the "Commissione di Inchiesta" the velocity had reached 20 cm per day by October 9. Compared with the final velocity of the sliding mass (about 25 m/sec), all movement, even the last phase, must be considered a creeping movement up to the very instant of the slide itself. . .

Starting from *Müller*'s [1964] statement, we will show that the following scenario of events is realistic for the Vaiont slide: during most of the creeping phase, the "rigid" body slides over a thick clay-rich layer (the shear zone) with inappreciable acceleration fed by the thermal feedback (a process we call thermally driven drifting creep). At this stage, shear heating is insufficient to trigger pressurization. Eventually, the slide becomes critical, since the shear heating localizes in a continuously shrinking zone. Localization of the shear heating is a consequence of the evolution of the heat production due to friction inside the shear zone, as described by the dissipation function (equation (22)). According to equation (22), once shear heating localizes in the shear band, essentially adiabatic boundary conditions are progressively established, and the temperature in the core of the shear zone increases to the critical pressurization temperature for "normally" consolidated clays. After the onset of pressurization, the process evolves explosively. Almost undrained conditions set in, leading rapidly to total loss of strength of the clay inside an ultrathin shear band at the base of the slide. At the end of this section, we will compare the results of our analysis with those from others.

4.1. Thermally Driven Drifting Creep

4.1.1. Blowup Time Estimate

[39] Following *Dold* [1985], the natural way of approaching the "Frank-Kamenetsky equation" analytically is to devel-

op a coordinate-perturbation analysis, using a suitable variable grouping to represent the spatial concentration of the effects of the exponential term in equation (24). Accordingly we discuss here the first-order asymptotic solution for the temperature $\theta(z, t)$ (see Appendix C),

$$\theta^* = \theta_0^* - \ln\left(\mathrm{Gr}(t_I^* - t^*) + \frac{z^{*2}}{4(a - \ln(t_I^* - t^*))}\right) \tag{26}$$

where t_I^* is the dimensionless blowup time, θ_0^* the initial dimensionless temperature at the center of the shear zone, and a is a constant defined by the initial conditions. To have a solution that depends continuously on the initial data, equation (26) must satisfy the condition of having always a maximum at $z = 0$. Thus a necessary restriction for the parameter a is

$$a = a_0 + \ln(t_I^*), \quad 0 < a_0 \ll 1. \tag{27}$$

The initial condition at the center of the shear zone provides an estimate for the dimensionless blowup time:

$$t_I^* = \frac{1}{\mathrm{Gr}} \gg 1. \tag{28}$$

Thus the Gruntfest number Gr is also from the physical point of view a crucial parameter of the problem. The real (dimensioned) blowup time that corresponds to equation (28) is evaluated using equation (25),

$$t_I = \frac{j(\rho C)_m}{m\dot{\gamma}_0 \bar{\tau}_{d,0}}. \tag{29}$$

We observe that, for a given strain rate, the lifetime of the creping slide decreases with increasing $\bar{\tau}_{d,0}$; it follows that "deep" catastrophically creeping landslides are more short-lived than shallow ones, since the shear stress increases with depth.

[40] Using the adiabatic approximation of equation (24), *Gruntfest* [1963] arrived at the blowup time estimate of equation (28), that is used also by *Leroy and Molinari* [1992] in their stability analysis of shear flows of non-Newtonian fluids. We notice that equation (28) is equally applicable to creeping landslides, where the deformation in most cases turns to be localized inside a narrow zone of intense shear. In landslides the actual lifetime of the creeping phase is bounded by the time at which the temperature reaches the pressurization limit. The onset of pressurization leads to catastrophic reduction of the strength of the gouge (see section 1). The critical temperature at which pressurization sets in is characteristic for a clay that has the ability to absorb or expel water (section 3.1). Clays with a pronounced tendency to swell in the presence of water may dehydrate in case of shear heating. To estimate the critical pressurization time, one should know material parameters such as the thermal softening coefficient, the heat capacity of the clay and the initial temperature at the core of the shear zone.

[41] At the critical pressurization time the slide enters an explosive phase that results in catastrophic acceleration. However, the process seems to turn critical even before this time. To justify this claim we study more closely the profile of local dissipation inside the shear zone (equation (24))

$$D^* = \mathrm{Gre}^{\theta^*}. \tag{30}$$

In fact, as time progresses the dissipation localizes within an ever shrinking core region, accompanied by a spectacular increase of the heat produced (Figure 4). The width of the shrinking zone is identified here by the point where the curvature is maximum, as the solution of the equation

$$\frac{\partial^3 D^*}{\partial z^3} = 0 \quad \Rightarrow \quad z_{cr}^* = \pm 2\sqrt{(a - \ln((t_I^* - t^*)(1 - \mathrm{Grt}^*))} \tag{31}$$

The critical progressive localization time t_{ip}^*, at which the dissipation starts localizing inside the shear zone, is computed from the condition $z_{cr}^* = \pm 1$ and it is expressed in terms of the Lambert W function [*Corless et al.*, 1996; *Barry et al.*, 2000],

$$t_{ip}^* \approx \left(1 + \frac{1}{4\mathrm{LambertW}\left(-1, -\frac{1}{4}\right)}\right) t_I^*. \tag{32}$$

Past the critical progressive localization time the temperature rises rapidly in the shrinking core region of the shear zone, thus leading to a runaway instability of shear localization in a plane (since equation (31) yields for $t^* \to t_I^*$ that $z_{cr}^* \to 0$). This observation allows us to claim that for times past the critical time $t_{ip}^* \approx 0.88\ t_I^*$ (corresponding to a real time of $t_{ip} \approx 148$ days, that is about 21 days before the final collapse of the Vaiont slide) the shear zone becomes significantly hotter, a process we could call "shear heating localization." As the lifetime limit t_I^* is approached, the core region of maximum temperature shrinks, and the peak temperature value increases rapidly. The abrupt increase of the temperature influences significantly the time necessary for the heat produced in the core of the shear zone, progressively forcing the shearing process toward adiabatic conditions. Accordingly, the critical time threshold t_{ip}^* for shear heating localization is indicated in Figures 5 and 6 as the "progressive localization" threshold.

4.1.2. An Asymptotic Formula for the Slide Velocity

[42] As mentioned in the Introduction, a dense network of monitoring instruments where installed in the area of the Vaiont slide, making it one of the better monitored slides ever. In addition, *Tika and Hutchinson* [1999] performed ring shear experiments in clay samples from Vaiont's sliding surface and reported that this clay exhibits slip and velocity weakening. However, the experiments where performed at slip rates greater than ~ 2 cm d^{-1}, which is about 10–100 times larger than those achieved during the creeping phase of the Vaiont slide and correspond to the movement of the slide during the last weeks (Figure 6). Therefore many parameters that are necessary for the present analysis were not measured in the field or evaluated through experiments. For this reason, in the Appendix D we perform a back analysis to obtain a set of material parameters, summarized in Table 2. The most important results of the analysis are the estimates of (1) the thickness of the shear zone, $d_S \approx 16.1$ cm, which is within the 0.5–17.5 cm thickness of the clay-rich layers (see section 2), and (2) the

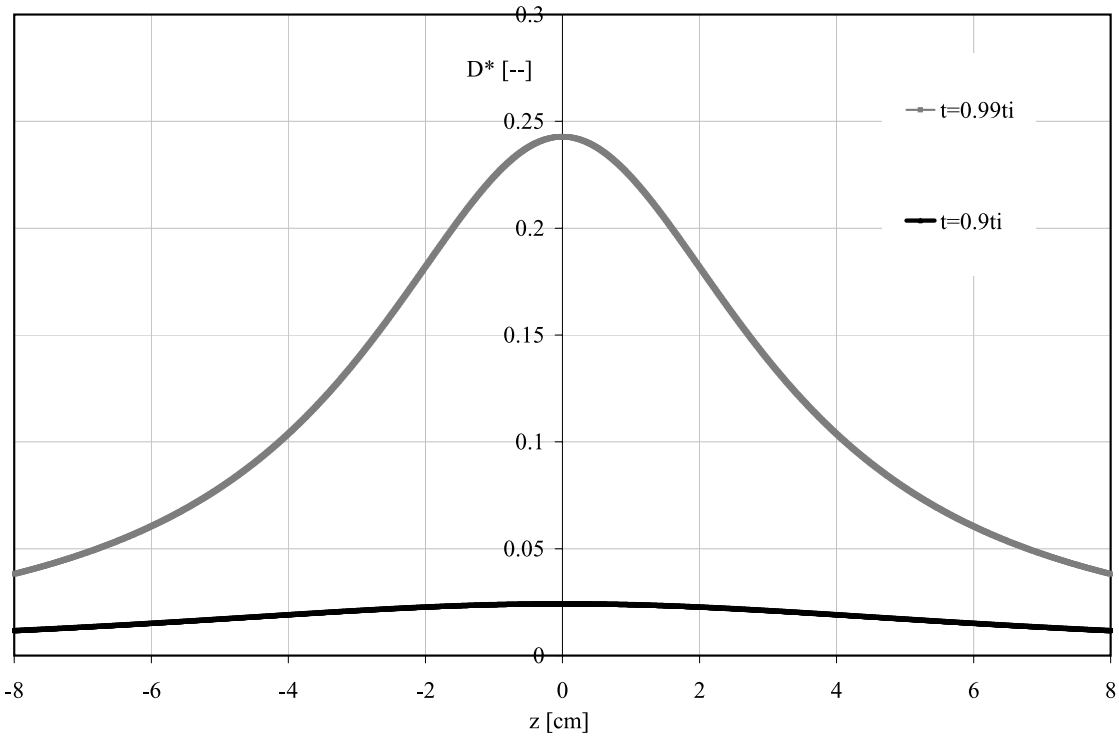

Figure 4. Distribution of the dissipation rate inside the shear zone past the critical time. Progressive localization occurs in a shrinking core region of intense heating.

blowup time, t_I = 169 days, which was calculated by using the hyperbolic law of *Sornette et al.* [2004], equation (1).

[43] Having established our input parameters, we may compute the velocity field inside the shear zone, using equation (19) for the shear strain rate and the asymptotic formula for the temperature field, equation (26). Demanding continuity of the velocity field at the common boundary of the two structures, we finally obtain the following function that describes the complete evolution of the sliding block velocity during the thermally driven creeping phase considered,

$$V(t^*) = 2d_S\dot{\gamma}_0 e^{\theta_0^*}\sqrt{\frac{a-\ln s_1}{Gr\cdot s_1}}\arctan\left(\frac{1}{2}\frac{1}{\sqrt{Gr\cdot s_1(a-\ln s_1)}}\right),$$
$$s_1 = t_I^* - t^*. \quad (33)$$

We emphasize that the above function describes the phenomenon in a time interval where the velocity increases more than 4 orders of magnitude (Figure 6). The validity of our model will be tested by fitting this expression for the velocity of the sliding block to the measured data provided by *Müller* [1964].

[44] The initial velocity for the back calculated initial time is $V(0) \approx 0.01$ cm/d. To calibrate our model we need to determine the initial value of the temperature inside the shear zone, which was located at a depth of ~120 m. Unfortunately, temperature measurements at the sliding surface of the Vaiont do not exist. A reasonable value is the air temperature in April (~8°C) [*Besio*, 1992] plus the geothermal contribution (30°C km^{-1}) which yields ~12°C at a depth of 120 m. The best fit of the velocity data from *Müller* [1964] yields indeed an initial temperature of about $\theta_0(\pm d_S/2) \approx 14$°C for the end of April. The temperature evolution in the shear zone is shown in Figure 5 while the best fit of the velocity data is in Figure 6. Our model successfully reproduces the field data from *Müller* [1964], providing an analytical formula (equation (33)) for the velocity evolution.

4.2. Thermal Pressurization

[45] The sudden, "last minute" acceleration of the slide can be explained with an almost instantaneous rise of the pore pressure because of shear heating. When the temperature rose up to the critical pressurization temperature, the dehydration of the clay material led to an explosive pore pressure rise, up to the point of "full pressurization": the point where pore pressure reaches the value of the total normal stress, leading to fluidization of the shear band. Thus, in the present setting, where we assumed that the basal material was in critical state, that pore pressure was almost constant during the creeping phase and the interstitial flow absent, any influence of permeability variations or of pore pressure feedback due to the dilatant or contractant behavior of the shear zone material [*Iverson*, 2005] is excluded. The critical pressurization temperature is reached in the core of the shear zone, during the very last phase of the thermally driven creep motion (Figure 5). At this stage of incipient pressurization, the temperature profile cusps in the center of the zone (Figure 7) where the spatial blowup coordinate was arbitrarily chosen ($z_I = 0$). The corresponding velocity profile tends progressively and smoothly to the

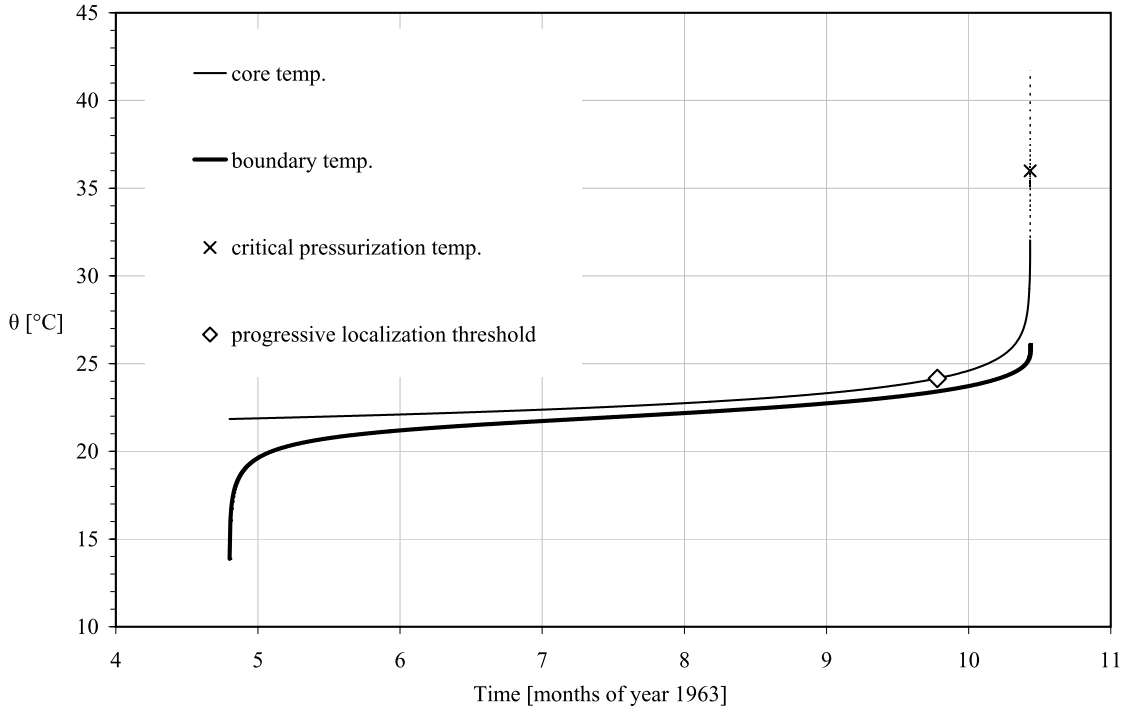

Figure 5. Temperature evolution at the core and at the boundary of the shear zone estimated for the accelerated-creep phase of the slide motion (equation (26)). Note the steep increase of the boundary temperature in the last week of April. During the following 5 months (the so-called thermally driven drifting creep) the core temperature increased ~3°C. Progressive localization of the shear heating initiated toward the end of September (white rhomb). During the first week of October, slip localization determined an abrupt rise of the temperature at the core of the shear zone, and the pressurization temperature (cross) was achieved a few minutes before the final collapse.

shape of a step function that is typical for a discontinuous slip across a plane, passing through the center of the shear zone. These profiles for the temperature and the velocity indicate a tendency of the deformation and heat generation to localize in a plane (i.e., a zero thickness shear zone). *Rice* [2006] produced a similar conclusion by considering the solution for the pressurization regime, when the momentum balance equation is considered. However, he showed that the solution of slip on a plane significantly overestimates the temperature field, and a model of slip on an infinitesimally small, but finite, shear band has to be considered instead. Here we showed that such a restriction sets in naturally, since the thermal pressurization takes place in a very thin (compared to the initial) band, formed by the progressive localization of the shear heating process inside the shear zone.

[46] The width of the shear band where pressurization takes place has been determined (see Appendix D) by inserting in equation (D10) the time needed for the core of the shear zone to achieve the critical pressurization temperature. From equation (D10), the shear band thickness is ~2.5 mm. *Vardoulakis* [2002a] assumed that the deformation is localizing inside a clay-rich zone with a thickness compatible with the thinnest deformation geostructure, namely that of a spontaneous shear band. The thickness of shear bands in kaolin clays from direct shear stress experiments is of few hundreds of microns [*Morgenstern and Tschalenko*, 1967]. In the same publication, the authors suggest a factor of 200 between the particle size and the shear band thickness, $d_B \approx 200 \cdot d_{50\%}$ (where $d_{50\%}$ is the mean particle diameter). If we adopt this relationship for the clay-rich layers of the Vaiont slide, we obtain an estimated shear band thickness $d_B \approx 1.4$ mm [*Vardoulakis*, 2002a], thus comparable to the shear band estimated thickness of 2.5 mm.

[47] The explosive character of the pressurization mechanism can be demonstrated by using the undrained adiabatic approximation of the governing equations (Appendix E). Since the excess pore pressure is zero for most of the creeping phase, we assume drained conditions until the shear band achieves the critical pressurization temperature θ_{cr} (see section 3.1). An indicative threshold for the instant t at which the adiabatic approximation of equation (5) describes the problem is when the timescale determined by the slip velocity becomes significantly greater than the characteristic time of the thermal diffusion process [*Garagash and Rudnicki*, 2003]. Indeed, we may introduce a characteristic timescale for thermal diffusion, $t_\kappa = d_S^2/\kappa_m$, and one for the slip rate, $t_s = d_S/V$. Using this method we may assume that adiabatic conditions are applied near the onset of the pressurization phase. In particular the point at which pressurization sets in (the "cross" in Figure 5)

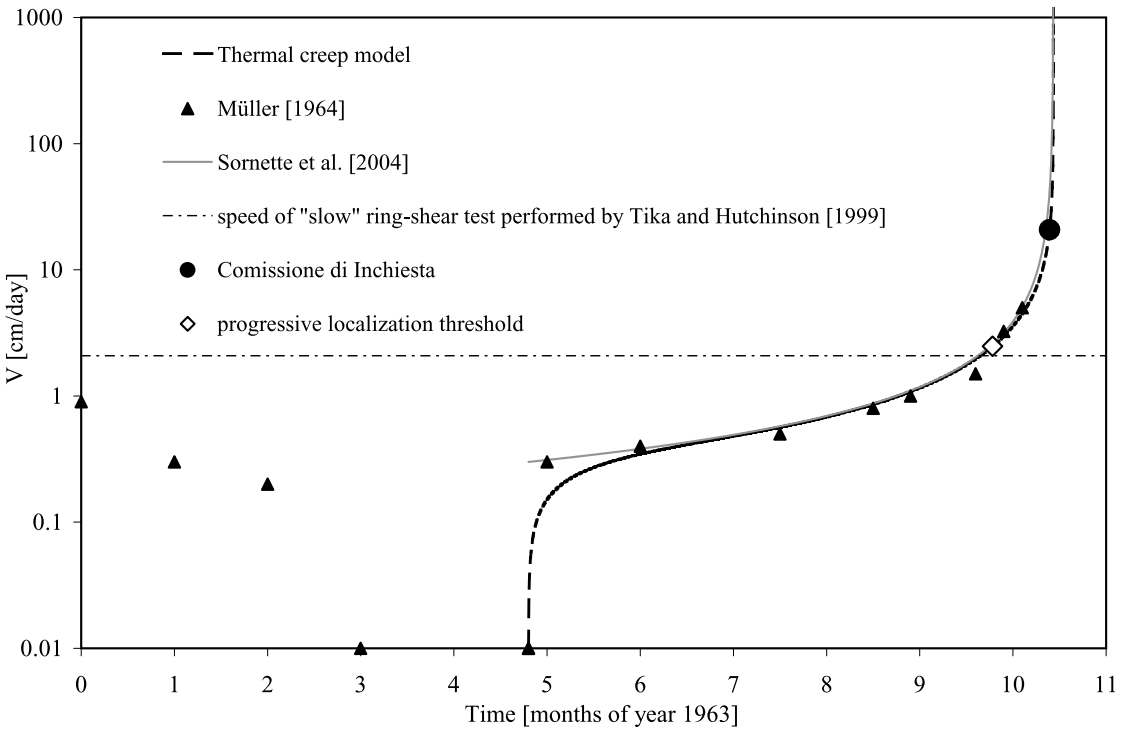

Figure 6. Fit of the velocity of the Vaiont slide during 1963. Field data are from *Müller* [1964] (triangles) and from the Commissione d'ichiesta as reported by *Müller* [1964] (circle at V = 20 cm/d). The latter was collected on the same day of the Vaiont final collapse. Field data fit was done using the hyperbolic law of *Sornette et al.* [2004] (equation (1), shaded line) and with the thermoviscoplastic creep model we propose (equation (31), dashed line). The horizontal dotted-dashed line indicates the velocity (2 cm/d) at which *Tika and Hutchinson* [1999] performed the ring shear tests on the clays from the sliding surface of Vaiont. The white rhomb denotes the time at which progressive localization of the shear heating was initiated and, as a consequence, the slide become critical.

corresponds to a ratio of about 1000 between the two timescales. Therefore we will assume for simplicity that the adiabatic approximation, along with undrained conditions, set in instantaneously at the onset of the pressurization phase, in a shear band of constant thickness.

[48] We assume that during this phase all the displacement and velocity induced friction softening, reported by *Tika and Hutchinson* [1999] (see section 4.1.2), occurs. For simplicity we will also assume that this softening happens almost instantaneously at the onset of the pressurization phase [*Vardoulakis*, 2002a]. Accordingly the friction coefficient is set constant throughout this phase and equal to the so call "fast residual" value ($\mu_{res} \approx 0.1$). Inertia becomes significant in this phase, however, the momentum equation,

$$\frac{\partial \tau}{\partial z} = \rho_m \frac{\partial v}{\partial t} \tag{34}$$

indicates that inside the shear band the shear stress is constant [*Rice*, 2006; *Sulem et al.*, 2007], $\tau \approx \tau_d(t)$. Indeed, if we assume a maximum value for the acceleration of $(1/2)g' \approx 1$ m/sec^2, and $\rho_m \approx 2.4$ gr/cm^3, then the maximum variation of the shear stress across a shear

Table 2. Material Parameters for Vaiont

Parameter	Value	Units	Source
σ_0	3.7	MPa	*Vardoulakis* [2002a]
$p_{ref} = \sigma'_0$	2.4	MPa	*Vardoulakis* [2002a]
τ_{eq}	0.97	MPa	
δ	15.2°	[]	
μ_{cs}	tan(22.2°)	[]	*Hicher* [1974]
μ_{res}	tan(10.2°)	[]	*Tika and Hutchinson* [1999]
$\dot{\gamma}_0$	$2.1 \cdot 10^{-7}$	s^{-1}	equation (D9)
N	0.01	[]	Appendix A
M	0.0093	[]	Appendix A
m	0.93	°C^{-1}	Appendix A
θ_1	22	°C	
d_S	16.1	cm	equation (D7)
jk_m	0.45	J (°C m s)$^{-1}$	*Vardoulakis* [2002a]
$j(\rho C)_m$	2.84	MPa °C^{-1}	*Vardoulakis* [2002a]
κ_m	$1.6 \cdot 10^{-7}$	m^2 s^{-1}	Appendix D
Gr	0.0028	[]	equation (23)
c_V	$7.3 \cdot 10^{-8}$	m^2 s^{-1}	*Vardoulakis* [2002a]
$\bar{\lambda}_m$	0.07	MPa °C^{-1}	*Vardoulakis* [2002a]
U	50.7	cm	Appendix D
t_I	169	days	Appendix D

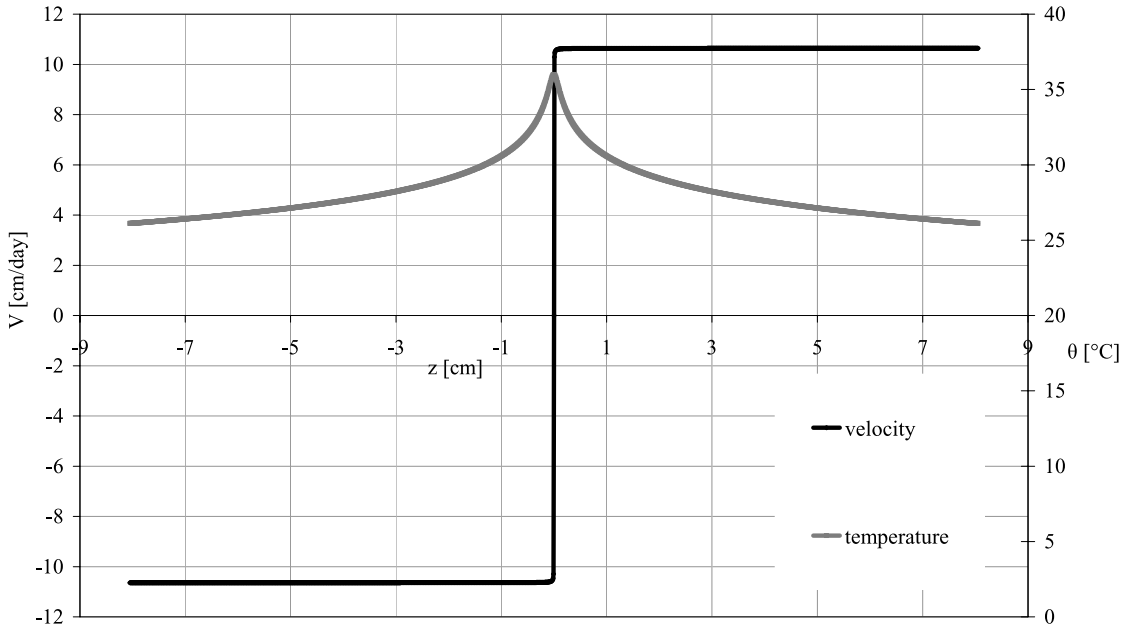

Figure 7. Velocity (left ordinate, solid line) and temperature (right ordinate, shaded line) profiles in the 16 cm thick shear zone (equation (D2)) at the instant when the temperature in the core of the shear zone reaches the critical pressurization value.

band d_B 1.4 mm thick is of the order of 1.5 Pa and thus negligible. In this framework, the evolution with time of the excess pore pressure and the temperature are described by

$$\Delta p = \sigma_0' \left[1 - \exp\left(- \left[\frac{t}{t_{ch}} \right]^2 \right) \right] \tag{35}$$

$$\theta = \theta_{cr} + \frac{\Delta p}{\lambda_m} \tag{36}$$

where θ_{cr} is the temperature at the center of the shear band at the onset of pressurization, whereas t_{ch} is the characteristic time controlling the rate of pressurization:

$$t_{ch} = \sqrt{\frac{j(\rho C)_m}{\lambda_m \mu_{res}} \frac{2 d_B}{g'}} \tag{37}$$

A similar expression has been used for the slip weakening due to thermal pressurization during earthquakes [*Wibberley and Shimamoto*, 2005].

[49] In Figure 8 we show the evolution of excess pore pressure (equation (35)) and temperature (equation (36)). The two equations provide a lower bound for the duration of the pressurization process and an upper bound for the temperature rise, since the (maximum) temperature at the end of this process is

$$\theta_{max,p} = \theta_{cr} + \frac{\sigma_0'}{\lambda_m} \approx 70.2^\circ C. \tag{38}$$

The maximum temperature achieved depends in general on the pressurization coefficient and the normal effective stress, and can vary from some tens to hundreds degrees. From equation (38), vaporization is excluded in the case of the Vaiont slide.

4.3. Comparison of the Blowup Time Estimate With Other Studies

[50] *Sornette et al.* [2004] verified the proposition of *Voight* [1988] that using the (Λ-t) model one could make a 10-day forecast for the Vaiont collapse. Also, these authors extended their study by using a Dieterich-Ruina friction model to obtain a hyperbolic relationship between the velocity of the slide and the collapse time. In our study, we showed that the thermal weakening model could yield an expression for the velocity of the slide, equation (33). This expression can reproduce the hyperbolic relationship of Sornette et al., equation (1), since as time approaches blowup equation (33) yields

$$V \approx d_S \dot{\gamma}_0 e^{\theta_0^*} \tilde{F}(t) \tag{39}$$

where

$$\tilde{F} = 2 \sqrt{\frac{1}{1 - t/t_l} \ln\left(\frac{1}{1 - t/t_l} \right)} \arctan\left(\frac{1}{2} \frac{1}{\sqrt{(1 - t/t_l) \ln\left(\frac{1}{1 - t/t_l} \right)}} \right). \tag{40}$$

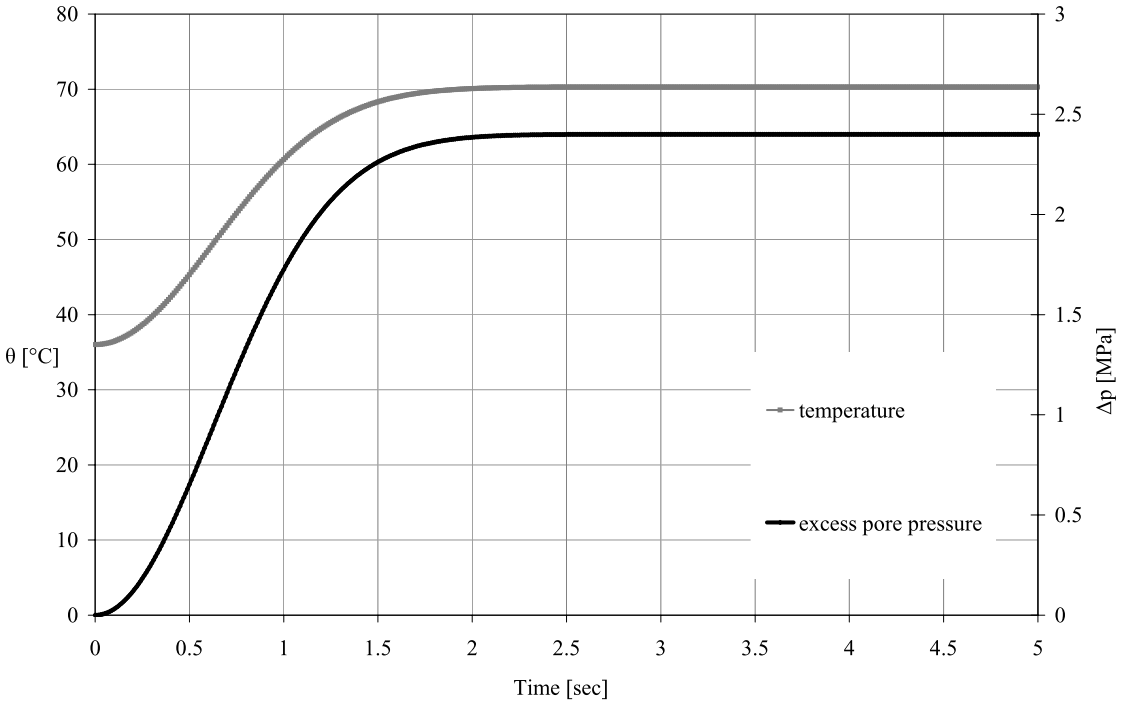

Figure 8. Temperature (left ordinate, shaded line) and excess pore pressure (right ordinate, solid line) evolution with time in the core of the shear zone according to equations (34) and (35) (i.e., undrained adiabatic approximation). Note that both temperature and pore pressure achieve their maximum value within ~2.5 s from the ignition of the thermal pressurization.

The above function can be always approximated by a power law function of the form

$$\tilde{F} \approx \frac{C_1}{\left(1 - \frac{t}{t_1}\right)^n}. \tag{41}$$

The parameters C_1 and n of the above approximation depend on the selected interval of time, where the optimization is performed (in the specific case $n \approx 1$). This means in turn that the formula for the slide velocity proposed by *Sornette et al.* [2004] is a good approximation of the theoretical one, equation (33) (Figure 6), and should be used for a first estimate of the relevant model parameters, as this was done in Appendix D.

[51] Although the two models seem to adopt different constitutive laws (an exponential feedback versus a logarithmic dependency), one could adapt the Dieterich-Ruina law to the shearing of a gouge of finite width by replacing the slip rate $\dot{u}$ by the shear strain rate $\dot{\gamma} \approx \dot{u}/d_S$, thus yielding for the local shear dissipation the following expression:

$$D_{loc} \approx \tau_d \dot{\gamma} = \tilde{D}_0 \left(\frac{\theta}{\theta_1}\right)^{\tilde{m}}, \quad \tilde{m} = -\frac{B}{A} \tag{42}$$

where $\tilde{D}_0 = \tau_d \dot{\gamma}_0$ and θ is a state variable. In this way, instead of an exponential thermal feedback, we obtain a power law thermal feedback as soon as $B < 0$ and $A > 0$, or vice versa. As stated also by *Helmstetter et al.* [2004], $B < 0$ applies to the frictional shearing of some rocks at hydrothermal conditions [*Blanpied et al.*, 1995]. *Sornette et al.* [2004] provide some stability regimes for the several values of the key parameter $\tilde{m}$. Using this approach we may equally obtain stability regimes, since for $\tilde{m} > 1$ the process leads to a finite time singularity for the velocity. This is consistent with the work of *Galaktionov and Vazquez* [2002] and *Fujita* [1969] in which they notice that the partial differential equation

$$\frac{\partial \theta}{\partial t} = \nabla^2 \theta + G\theta^{\tilde{m}}, \quad G > 0 \tag{43}$$

behaves in a similar way with the Frank-Kamenetsky equation, presenting blowup for $\tilde{m} > 1$. Therefore, if we define the temperature as the state variable θ in the Dieterich-Ruina law, then the energy balance equation, equation (5) along with equation (42) would yield the equation (43), thus the two models could provide similar results.

5. Conclusions

[52] The potential contribution of frictional heating of the pore water and the effect of thermal pressurization in the catastrophic loss of strength that occurred in Vaiont slide has been studied by several authors [*Anderson*, 1980; *Voight and Faust*, 1982; *Hendron and Patton*, 1985; *Vardoulakis*, 2002a]. The onset of thermal pressurization has been also claimed in earthquake science to explain dynamic fault weakening during coseismic slip [e.g., *Rice*, 2006]. In this

paper we presented an analysis of both the long creeping and the final pressurization phases of a creeping landslide. We showed that frictional heating may eventually trigger the explosive pressurization phase, not in a sudden and unexpected way, but rather smoothly. The final slide collapse may be predicted by means of a one dimensional model that accounts for the heat production induced by friction at the base of the slide. The model provides a formula (equation (33)) for the velocity of the slide, which might be useful for hazard evaluation. In the case of the Vaiont slide, the formula fits the natural data up to 169 days before the final collapse (Figure 6).

[53] With the present model the concept of the "shear heating localization" phase of the creeping motion was naturally introduced and calculated to have started about 21 days before the collapse. During this phase, the shear zone is entering a (thermally) self-shielding process, which takes place in a continuous shrinking-core region where the dissipation localizes. Self-shielding forces the shearing process in the clay-rich layer toward adiabatic conditions, and determines the abrupt temperature rise that triggers the pressurization phase. As a consequence, a $\sim$1–2 mm thick shear band is formed at the transition from the critical (creeping phase) to the residual (pressurization phase) state; in this thin layer, pore pressure increases to its maximum value leading to its complete fluidization.

[54] Though it includes some simplifications (assumptions 1–5 as described in section 1), the thermoporomechanical model presented in this paper might become a useful tool to forecast the blowup time for creeping landslides. However, it demands, together with detailed geological investigations (e.g., dip of the sliding surface, thickness, composition and temperature monitoring near or at the shear zone) the determination of several material parameters, such as the thermal softening coefficient, M, the strain rate hardening coefficient, N, the specific heat, C_m, the pressurization coefficient, λ_m and the reduction of the critical friction angle with temperature for hydrating clays. To make model predictions reliable, these parameters have to be calibrated using data from thermoporomechanical experiments performed at deformation conditions and slip rates similar to those in nature and also to be bounded by back analyses that are using inputs from carefully monitored slides.

Appendix A: Generalization of Bagnold's Model

[55] In order to make clear the choice of the particular values for the parameters M and N, appearing in the thermoviscoplastic friction law, equation (17), we refer here the rheological law formulated by *Bagnold* [1954] for noncolloidal suspensions of insoluble particles. We recall that, depending on the flow regime (fast or slow shear flow), Bagnold's law for the shear stress can be written as follows:

$$\tau \approx \begin{cases} 2.25\lambda_B^{3/2}\dot{\gamma}\,\rho_w\nu_w & \text{(slow flows)} \\ 0.26\lambda_B^{7/4}D_g\dot{\gamma}^{3/2}\sqrt{\rho_s\rho_w}\sqrt{\nu_w} & \text{(fast flows)} \end{cases} \tag{A1}$$

where ρ_w and ν_w are the density and the kinematic viscosity of water, ρ_s and D_g are the particle density and diameter, and λ_B is a factor that depends on the concentration of the particles in the mixture. We remark also that the viscosity of water is temperature-dependent, and its impact in Bagnold's law, equation (A1) is

$$\nu_w = \nu_{ref}e^{-M_w(\theta-\theta_{ref})}$$
$$\nu_{ref} = 0.957\ \text{mm}^2/\text{sec}, \quad \theta_{ref} = 22^\circ\text{C}, \quad M_w = 0.021^\circ\text{C}^{-1} \tag{A2}$$

or

$$\sqrt{\nu_w} = \sqrt{\nu_{ref}}e^{-\frac{M_w}{2}(\theta-\theta_{ref})}$$
$$\sqrt{\nu_{ref}} \approx 0.98\ \text{mm}^2/\text{sec}, \quad \theta_{ref} = 22^\circ\text{C}, \quad \frac{M_w}{2} \approx 0.01^\circ\text{C}^{-1} \tag{A3}$$

In other words the exponent M in equation (17) reflects the temperature dependence of water viscosity.

[56] Strain rate friction hardening in equation (17) is viewed here as the necessary counterbalancing effect to thermal softening. In order to estimate the strain rate sensitivity exponent N we resorted to experimental results concerning kaolin clay, reported by *Leinenkugel* [1976] and, thus yielding $N \approx 0.01$ [*Vardoulakis*, 2002b]. This value for the strain rate creep exponent is also applied successfully in the prediction of the retarding action of dowels in steadily creeping slopes in clayey soils [*Schwartz*, 1987]. As we saw in the text, the critical parameter is the exponent ratio of the temperature sensitivity coefficient over the strain rate sensitivity coefficient, m = M/N. A parameter analysis of *Vardoulakis* [2002b] has shown that indeed the value $m \approx 1^\circ\text{C}^{-1}$ is realistic.

Appendix B: Linear Stability Analysis of the Steady State Solution

[57] The state solution of equation (24) is [*Chen et al.*, 1989; *Leroy and Molinari*, 1992; *Vardoulakis*, 2002b]

$$\theta^*(z) = \theta_d^* - 2\ln\left(\frac{\cosh(\alpha z^*)}{\cosh\alpha}\right) \tag{B1}$$

where θ_d^* is the temperature at the boundary (see Figure 2b), and

$$\alpha = \sqrt{\frac{Gr}{2}}e^{\frac{\theta_{max}^*}{2}} \tag{B2}$$

The exact solution for the critical boundary temperature, where the steady state presents a bifurcation point, was derived by *Chen et al.* [1989]

$$\theta_{d,cr}^* = \ln\left(\frac{2}{\sinh^2(\alpha_{cr})\cdot Gr}\right) \tag{B3}$$

where the critical value for the parameter α is given by the following transcendental equation:

$$\alpha\ \tanh\alpha = 1 \quad \Rightarrow \quad \alpha_{cr} \approx 1.2 \tag{B4}$$

Notice that *Vardoulakis* [2002b] provided an estimate for the critical value $\alpha_{cr} = 1$ by performing a similar bifurcation

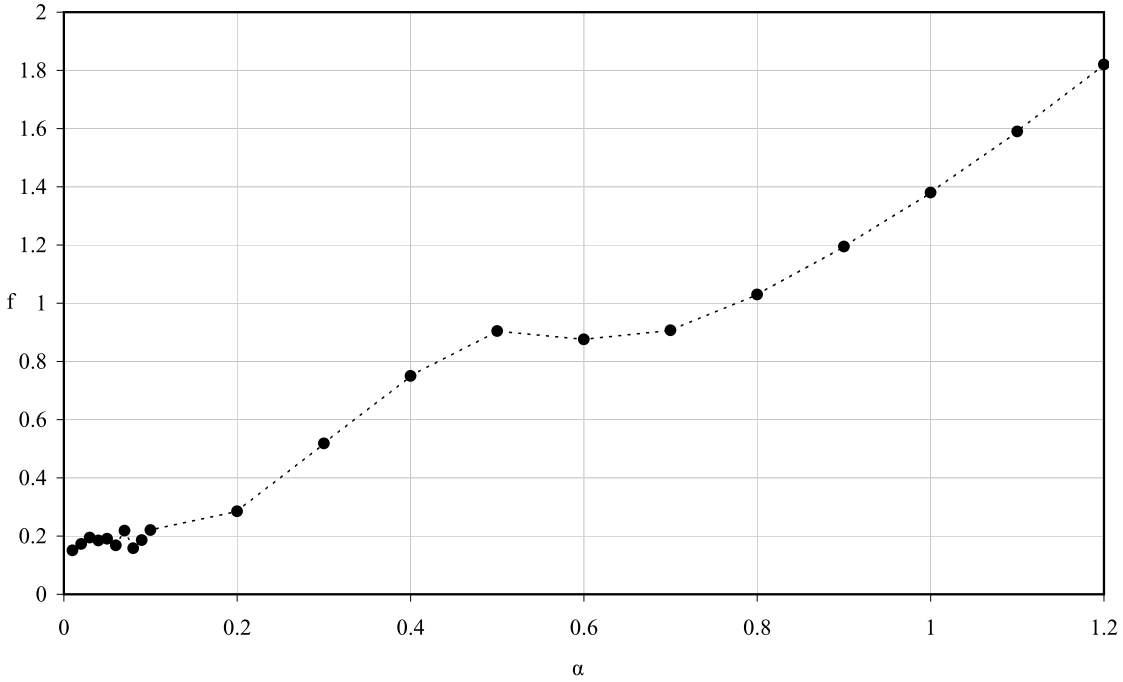

Figure B1. Numerical determination of the growth coefficient of the perturbation as a function of the forcing parameter. The growth coefficient, f, admits only positive values for any value of the forcing parameter, α, which is a function of the core temperature. Thus the steady state solution is linearly unconditionally unstable.

analysis using the, not so well known, LambertW functions [*Corless et al.*, 1996; *Barry et al.*, 2000].

[58] As it turns out in real geomechanical applications as the present one where the shear stress remains practically constant, the steady state solution has little significance, since, as we will outline next, the steady solution is linearly unstable. To demonstrate this we consider a solution of the transient problem, equation (24), under the assumption that the shear stress is constant. This means that unlike the analysis of *Chen et al.* [1989] the momentum equation does not enter into our analysis. This solution of the transient equation is constructed as a perturbation of the steady state solution,

$$\theta^* = \theta_e^*(z^*) + \tilde{\theta}(z^*, t^*) \tag{B5}$$

where

$$\theta_e^*(z^*) = \theta_{max}^* - 2\ln(\cosh(\alpha z^*)) \tag{B6}$$

thus yielding

$$\frac{\partial \tilde{\theta}^*}{\partial t^*} = \frac{\partial^2 \tilde{\theta}^*}{\partial z^{*2}} + \mathrm{Gr}\, e^{\theta_e^*}\left(e^{\tilde{\theta}^*} - 1\right) \tag{B7}$$

Within the frame of a linear stability analysis the amplitude of the perturbation is assumed to be small, thus equation (B7) with equation (B6) and equation (B5) yields

$$\frac{\partial \tilde{\theta}^*}{\partial t^*} = \frac{\partial^2 \tilde{\theta}^*}{\partial z^{*2}} + \frac{2\alpha^2}{\cosh^2(\alpha z^*)}\tilde{\theta}^* \tag{B8}$$

With

$$\tilde{\theta}(z^*, t^*) = F(\xi)\exp(ft^*), \quad \xi = \alpha z^* \tag{B9}$$

we obtain the following ordinary differential equation:

$$\frac{d^2F}{d\xi^2} + \left(\frac{2}{\cosh^2\xi} - \frac{f}{\alpha^2}\right)F = 0 \tag{B10}$$

The solution of the resulting ordinary differential equation is given in terms of Legendre functions,

$$\begin{aligned} F &= \sqrt{\cosh\xi}\,(C_1 LP(\alpha, f, z^*) + C_2 LQ(\alpha, f, z^*)) \\ LP(\alpha, f, z^*) &= \mathrm{LegendreP}\left(u, \frac{3}{2}, \sqrt{1-\cosh^2\xi}\right) \\ LQ(\alpha, f, z^*) &= \mathrm{LegendreQ}\left(u, \frac{3}{2}, \sqrt{1-\cosh^2\xi}\right) \\ u &= \frac{1}{2}\left(\frac{2\sqrt{s}}{\alpha} - 1\right) \end{aligned} \tag{B11}$$

The perturbation field must satisfy homogeneous boundary conditions,

$$\tilde{\theta}(\pm 1, t^*) = 0 \tag{B12}$$

this leads to the following condition for the growth coefficient of the perturbation,

$$\mathrm{Det}(\alpha, f) = \left(\Re e(P_1)^2 + \Im m(P_1)^2\right) - \left(\Re e(Q_1)^2 + \Im m(Q_1)^2\right) = 0 \tag{B13}$$

where

$$P_1 = LP(\alpha, f, 1), \quad Q_1 = LQ(\alpha, f, 1) \tag{B14}$$

If we resolve numerically the above equation, equation (B13), we get that $f > 0$ is an increasing function of the forcing parameter α (Figure B1). This proves that the steady state solution is unstable for all α, in the domain of its existence.

[59] An unconditionally linearly unstable steady state solution indicates that any small perturbation of the steady state temperature profile would inevitably lead to a finite time blowup. A finite time blowup occurs when the solution becomes infinite at some "ignition" point (or points) z_I, as time t approaches a certain finite time t_I. This means that in this case there exists a time t_I ($0 < t_I < \infty$), called the blowup time, such that the solution is well defined for all $0 < t < t_I$, within a bounded domain, while the temperature tends to infinity, at least at a point inside the band, as time approaches the critical blowup time ($t \to t_I$).

Appendix C: Coordinate-Perturbation Analysis

[60] We assume that the blowup is "ignited" at the center of the shear band ($z_I = 0$), since the temperature is assumed to present maximum at this spatial point. Therefore we demand also that our model should yield a profile that has a maximum at the origin as an initial condition:

$$\theta^*(0,0) = \theta_0^* \tag{C1}$$

where θ_0^* is the (maximum) dimensionless temperature at the center of the shear zone. In order to seek asymptotic solutions for this Cauchy (initial value) problem, we follow here *Dold*'s [1985] suggestion for the most robust variable transformation:

$$\begin{aligned} \xi &= -\ln(t_I^* - t^*) \\ \eta &= \frac{z^*}{\sqrt{-\xi e^{-\xi}}} \\ E &= e^{\xi - \Theta} \\ \Theta &= \theta^* - \theta_0^* \end{aligned} \tag{C2}$$

If we substitute these expressions in our initial equation and apply the framework proposed by Dold, we find that E satisfies the partial differential equation:

$$E_\xi + \frac{1}{2}\eta E_\eta + Gr = E + \xi^{-1}\left[\frac{\eta}{2}E_\eta + E_{\eta\eta} - \frac{E_\eta^2}{E}\right] \tag{C3}$$

E can be written as

$$E = E_1(\eta) + \frac{\ln\xi}{\xi}E_2(\eta) + \frac{1}{\xi}E_3(\eta) + \frac{\ln\xi}{\xi^2}E_4(\eta) + \frac{1}{\xi^2}E_5(\eta) + O\left(\frac{\ln^2\xi}{\xi^3}\right) \tag{C4}$$

This immediately results in for the first-order term

$$\frac{1}{2}\eta\dot{E}_1 + Gr = E_1 \tag{C5}$$

Its solution is

$$E_1 = Gr + c_1\frac{\eta^2}{4} \tag{C6}$$

The second-order term must satisfy

$$\frac{1}{2}\eta\dot{E}_2 = E_2 \tag{C7}$$

So

$$E_2 = c_2\frac{\eta^2}{4} \tag{C8}$$

For the third-order term we have

$$\frac{1}{2}\eta\dot{E}_3 - E_3 = \ddot{E}_1 + \frac{1}{2}\eta\dot{E}_1 - \frac{\dot{E}_1^2}{E_1} \tag{C9}$$

giving

$$E_3 = c_1\frac{\eta^2}{4}\left[c_3 + \ln\left(Gr + c_1\frac{\eta^2}{4}\right)\right] - \frac{c_1}{2} + (1-c_1)c_1\frac{\eta^2}{4}\ln\left(\frac{\eta^2}{Gr + c_1\frac{\eta^2}{4}}\right) \tag{C10}$$

Since the thermal runaway is spatially varying, c_1 cannot have the value zero. Thus, unless c_1 has the value unity, the final term in the above expression will have a singular second derivative. This is clearly unacceptable since there are no singularities in the development of θ before the blowup time is reached. It follows that

$$c_1 = 1 \tag{C11}$$

So, equation (C4) can be written as

$$E = Gr + \frac{\eta^2}{4} + \frac{\ln\xi}{\xi}\frac{\eta^2}{4} + \frac{1}{\xi}\left\{\frac{\eta^2}{4}\left[c_3 + \ln\left(Gr + \frac{\eta^2}{4}\right)\right] - \frac{1}{2}\right\} + O\left(\frac{\ln\xi}{\xi^2}\right) \tag{C12}$$

In the original coordinates, the above expression can be written

$$\theta^* - \theta_0^* = \xi - \ln\left(Gr + \frac{\eta^2}{4}\right) - \frac{\ln\xi}{\xi}\frac{\frac{\eta^2}{4}}{Gr + \frac{\eta^2}{4}} + \frac{1}{\xi}\left\{\frac{1}{2} + \frac{\frac{\eta^2}{4}}{Gr + \frac{\eta^2}{4}}\left[c_3 - \ln\left(Gr + \frac{\eta^2}{4}\right)\right]\right\} + O\left(\frac{\ln\xi}{\xi^2}\right) \tag{C13}$$

If we keep the first order of equation (C13) the temperature field is given by

$$\theta^* - \theta_0^* = \xi - \ln\left(Gr + \frac{\eta^2}{4}\right) + O\left(\frac{\ln\xi}{\xi}\right) \tag{C14}$$

or

$$\theta^* = \theta_0^* - \ln\left[\mathrm{Gr}(t_I - t) + \frac{z^2}{4[a - \ln(t_I - t)]}\right] \tag{C15}$$

In his paper Dold generalizes the asymptotic expression (C13) by inserting into the initial group of transformations (C2) the generalized expression for η,

$$\eta = \frac{z^*}{\sqrt{(t_I^* - t^*)[a - \ln(t_I^* - t^*)]}} \tag{C16}$$

In the above expression, a is a parameter which is either constant or weakly time-dependent. It is used by Dold as a normalization factor for the variable grouping (C2), such that when $\zeta = a - \ln(t_I^* - t^*)$ and η are both of order one, $(t_I^* - t^*)$ and $(z^* - z_I^*)^2$ are both of order e^a (in our case of course $z_I^* = 0$). The solution (C15) that we constructed is proved to be a stable solution with respect to small perturbations of the initial conditions [*Bressan*, 1992; *Schochet*, 1999].

Appendix D: Parameter Estimation

[61] In this appendix we perform an inverse analysis in order to estimate the material parameters presented in the previous sections. We begin our analysis by noticing that a quite common approximation for the thermal behavior inside a shear zone is the adiabatic approximation. In our case the adiabatic approximation of equation (24) provides the following "crude" approximation of the temperature (see equation (26)):

$$\theta^* = \theta_0^* - \ln[\mathrm{Gr}(t_I^* - t^*)] \tag{D1}$$

By using this expression we will try to obtain a first estimate of the blowup time of Vaiont. If we assume the adiabatic approximation of the heat equation, as described above,

$$\frac{\partial\theta}{\partial t} \approx \frac{1}{j(\rho C)_m}\tau_d\dot{\gamma} \tag{D2}$$

and the approximation of a uniform strain rate field across the shear zone,

$$\dot{\gamma} \approx \frac{v_d}{d_S/2} \tag{D3}$$

then we get an estimation for the velocity at the boundary of the shear zone

$$v_d \approx 2\frac{jk_m}{m\tau_d d_S}\frac{\partial\theta^*}{\partial t^*} \tag{D4}$$

We remark that the boundary velocity v_d, measured with respect to the mid axis of the shear zone, is half the sliding velocity of the block (Figure 2),

$$V = 2v_d \quad \Rightarrow \quad v_d = \frac{1}{2}V(t) \tag{D5}$$

On the other hand, from equation (D1) we may calculate the temperature derivative entering in equation (D4), as follows:

$$\frac{\partial\theta^*}{\partial t^*} \approx \frac{1}{t_I^* - t^*} \tag{D6}$$

The slide velocity computed from equations (D4), (D5) and (D6) yields the estimate of *Sornette et al.* [2004]

$$V = U\frac{1}{t_I - t} \tag{D7}$$

where the parameter U is identified as

$$U = \frac{j(\rho C)_m}{m\tau_d}d_S \tag{D8}$$

[62] As already mentioned, the above adiabatic approximation will be used to provide us a first estimate for the blowup time of the Vaiont slide, as well as for the material properties of the creeping phase of the slide. Indeed, equation (D3) can be expressed for the sliding block as

$$\dot{\gamma}_0 \approx \frac{V(0)}{d_S} \tag{D9}$$

If we use the above equation and equation (D7) we obtain an estimate for the reference shear strain rate of the shear zone,

$$\dot{\gamma}_0 = \frac{U}{t_I d_S} \tag{D10}$$

Having a complete formula in our hands to begin with, equations (D7)–(D10), we can try to obtain a first lifetime estimate for the Vaiont. Indeed the best fit for *Müller*'s [1964] data, using the formula of *Sornette et al.* [2004], equation (D7), provides the following estimates (Figure 6):

$$\begin{aligned} t_I &= 169 \text{ day} \\ U &= V_0 t_I \approx 0.3\frac{\text{cm}}{\text{day}}t_I = 50.7\,\text{cm} \end{aligned} \tag{D11}$$

where V_0 is the initial velocity of the sliding block. From these estimates we assume that the accelerating slide creep motion in the Vaiont slide was initiated around the end of April 1963, as indicated in Figure 6.

[63] Using the mixtures' theory approximation for the specific heat of the clay, $(\rho C)_m = (1 - \phi)\rho_s C_s + \phi\rho_w C_w$, and the values for the porosity of the clay, as well as for the specific heat of the constituent as these are listed by *Vardoulakis* [2002a], we arrive at an estimate

$$j(\rho C)_m = 2.84\ \frac{\text{MPa}}{^\circ\text{C}} \tag{D12}$$

Notice that *Picard* [1994] gives the following value for the pertinent thermomechanical parameters of water-saturated clays: $j(\rho C)_m = 2.85$ MPa/°C. Starting from this value and the values of the parameter listed in equation (D11), which

were extracted from the field data, we arrive from equation (D8) at an estimate for the thickness of the shear zone, $d_S \approx 16.1$ cm. With this estimate for the thickness of the shear zone, and from equation (D10), we get an estimate of the parameter $\dot{\gamma}_0 = 2.1 \cdot 10^{-7}$.

[64] With the value for the Fourier coefficient of the Vaiont clay as given by *Vardoulakis* [2002b], $jk_m \approx 0.45$ J/(°Cms), we get for the Kelvin diffusivity coefficient, $\kappa_m = 1.6 \cdot 10^{-7}$ m^2/s. This value is relatively close to the one given by *Picard* [1994], $\kappa_m = 5.96 \cdot 10^{-7}$ m^2/s. Finally, from the above values and the definition of the Gruntfest number, equation (25) we estimate that, $Gr = 2.81 \cdot 10^{-3}$.

[65] For the complete calibration of the model, the parameter a is determined from the initial velocity [*Dold*, 1985]. Indeed, keeping in mind the restriction (27), we may set here that

$$a = a_0 + \ln(t_f^*), \quad 0 < a_0 \ll 1 \tag{D13}$$

Then from equation (33) we get

$$V(0) = \pi d_B \dot{\gamma}_0 e^{\theta_0^*} \sqrt{a_0} \tag{D14}$$

Thus for $V(0) \approx 0.01$ cm/day we get that $\sqrt{a_0} = 0.01$. The system and material parameters used here in are summarized in the Table 2.

Appendix E: Undrained Adiabatic Approximation

[66] The explosive character of the pressurization mechanism can be demonstrated by using the undrained adiabatic approximation of the governing equations. We assume that shear stress obeys a Coulomb friction law,

$$\tau_d = (\sigma_0' - \Delta p)\mu \tag{E1}$$

and that during the considered pressurization phase, the friction coefficient is constant and equal to the so call ''fast residual'' value, which according to *Tika and Hutchinson* [1999] and *Vardoulakis* [2002a] could be set as $\mu = \mu_{res} \approx \tan(10.2°)$.

[67] Consistent with the above is the assumption that all involved fields are practically only functions of time, which leads to the so-called undrained adiabatic approximation of the heat and pressurization equations,

$$\frac{d\theta}{dt} \approx \frac{\mu_{res}}{j(\rho C)_m}(\sigma_0' - \Delta p)\frac{V}{d_B} \tag{E2}$$

$$\frac{d\Delta p}{dt} \approx \lambda_m \frac{d\theta}{dt} \tag{E3}$$

Assuming continuity of the velocity at the shear band boundaries, the set of governing equations is closed with the equation that describes the accelerated slide motion,

$$\frac{dV}{dt} = g'\left(1 - \frac{\mu_{res}}{\tan\delta}\frac{\sigma_0' - \Delta p}{\sigma_0}\right) \tag{E4}$$

The following initial conditions apply for the new system of equations, equations (E2)–(E4):

$$t = 0: \quad V = 2v_{0,p}, \quad \theta = \theta_{0,p}, \quad \Delta p = 0 \tag{E5}$$

We eliminate the temperature from equations (E2) and (E3) and we introduce the following set of dimensionless variables:

$$T^* = \frac{t}{t_{ref}}, \quad p^* = \frac{\Delta p}{p_{ref}}, \quad V^* = \frac{V}{v_{ref}} \tag{E6}$$

where

$$t_{ref} = \sqrt{\frac{d_B}{g'}}, \quad v_{ref} = \sqrt{g' d_B}, \quad p_{ref} = \sigma_0' \tag{E7}$$

The resulting set of evolution equations is

$$\begin{aligned} \frac{dV^*}{dT^*} &= 1 - \alpha(1 - p^*) \\ \frac{dp^*}{dT^*} &= \beta'(1 - p^*)V^* \end{aligned} \tag{E8}$$

where

$$\begin{aligned} \alpha &= \frac{\mu_{res}}{\tan\delta}\frac{\sigma_0'}{\sigma_0} \approx 0.2 \\ \beta' &= \frac{\lambda_m}{j(\rho C)_m}\mu_{res} = 0.002 \end{aligned} \tag{E9}$$

If we neglect the transient effect on the slide acceleration, then from equation (E8) we get an approximation of the velocity and the excess pore pressure profiles

$$\frac{dV^*}{dT^*} \approx 1 \quad \text{and} \quad p^* \approx 1 - \exp\left(-\frac{\beta'}{2}T^{*2}\right) \tag{E10}$$

Notation

C_m	specific heat of the mixture, cal (g °C)$^{-1}$.
c_v	consolidation coefficient, m^2 s^{-1}.
c	compressibility of soil, 1/MPa.
d_S	shear zone thickness, m.
d_B	pressurization's shear band thickness, m.
g	acceleration of gravity, m s^{-2}.
Gr	Gruntfest number.
N	frictional rate-sensitivity coefficient.
m	Ratio of thermal and rate sensitivity coefficients, 1/°C.
M	Frictional thermal-sensitivity coefficient, 1/°C.
k_F	Fourier's thermal conductivity of the mixture, cal (°C m s)$^{-1}$.
k_{Fs}	Fourier's thermal conductivity of the solid particles (clay), cal (°C m s)$^{-1}$.
k_{Fw}	Fourier's thermal conductivity of the pore fluid (water), cal (°C m s)$^{-1}$.
OCR	overconsolidation ratio.
Δp	excess pore pressure, Pa.
Q	heat flux.

s_1 reverse time, s.
t time, s.
v velocity field inside the shear zone, m s^{-1}.
V velocity field of the sliding block, m s^{-1}.
t_I blowup time or landslide lifetime, s.
z coordinate normal to the shear band axis.
α Thermal expansion coefficient, 1/°C.
β Taylor Quiney's coefficient.
$\dot{\gamma}$ shear strain rate.
θ temperature field, °C.
θ_1 reference temperature, °C.
κ_m Kelvin's coefficient of thermal diffusivity of the soil-water mixture, m^2 s^{-1}.
λ_m pressurization coefficient, MPa $°C^{-1}$.
μ Coulomb friction coefficient.
ρ density of the soil-water mixture, g cm^{-3}.
σ'_n effective stress acting normal to the shear band axis, Pa.
τ_d shear stress at the interface between substructures, Pa.
ϕ porosity.

[68] **Acknowledgments.** This paper is a partial result of the Project Pythagoras I, within the framework of the Operational Program for Educational and Vocational Training (EPEAEK II), cofunded by the European Social Fund (75%) and National Resources (25%).

References

Anderson, D. L. (1980), An earthquake induced heat mechanism to explain the loss of strength of large rock and earth slides, in *Proceedings of the International Conference on Engineering for Protection From Natural Disasters*, pp. 569–580, John Wiley, New York.

Bagnold, R. A. (1954), Experiments on a gravity free dispersion of large solid spheres in a Newtonian fluid under shear, *Proc. R. Soc. London, Ser. A*, *225*, 49–63.

Barry, D. A., J.-Y. Parlange, L. Li, H. Prommer, C. J. Cuningham, and F. Stagnitti (2000), Analytical approximations for real values of the Lambert W-function, *Math. Comput. Simul.*, *53*, 95–103.

Belloni, L. G. and R. Stefani (1992), Natural and induced seismicity at the Vaiont slide, paper presented at Meeting on the 1963 Vaiont Landslide, Int. Assoc. for Eng. Geol., Ferrara, Italy.

Besio, M. (1992), Hydrogeological notes regarding Mount Toc and vicinity, paper presented at Meeting on the 1963 Vaiont Landslide, Int. Assoc. for Eng. Geol., Ferrara, Italy.

Blanpied, M. L., D. A. Lockner, and J. D. Byerlee (1995), Frictional slip of granite at hydrothermal conditions, *J. Geophys. Res.*, *100*, 13,045–13,064.

Bressan, A. (1992), Stable blow up patterns, *J. Differ. Equations*, *98*, 57–75.

Broili, L. (1967), New knowledge on the geomorphology of the Vaiont slide slip surface, *Rock Mech.*, *5*, 38–88.

Carloni, G. C., and R. Mazzanti (1964), Rilevamento geologico della frana del Vaiont, *G. Geol.*, *XXXII*, 105–138.

Chang, K. J., A. Taboada, M.-L. Lin, and R.-F. Chen (2005a), Analysis of landsliding by earthquake shaking using a block-on-slope thermo-mechanical model: Example of Jiufengershan landslide, central Taiwan, *Eng. Geol.*, *80*, 151–163.

Chang, K. J., A. Taboada, and Y. C. Chan (2005b), Geological and morphological study of the Jiufengershan landslide triggered by the Chi-Chi Taiwan earthquake, *Geomorphology*, *71*, 293–309.

Chen, H. T. Z., A. S. Douglas, and R. Malek-Madani (1989), An asymptotic stability condition for inhomogeneous simple shear, *Q. Appl. Math.*, *47*, 247–262.

Ciabatti, M. (1964), La dinamica della frana del Vaiont, *G. Geol.*, *XXXII*, 139–158.

Corless, R. M., G. H. Connet, D. E. G. Hare, D. J. Jeffrey, and D. E. Knuth (1996), On the Lambert W function, *Adv. Comput. Math.*, *5*, 329–359.

Delage, P., N. Sultan, and Y.-J. Cui (2000), On the thermal consolidation of Boom clay, *Can. Geotech. J.*, *37*, 343–354.

Dieterich, J. H. (1978), e-dependent friction and the mechanics of stick-slip, *Pure Appl. Geophys.*, *116*, 790–806.

Dieterich, J. H. (1992), Earthquake nucleation on faults with rate- and state dependent strength, *Tectonophysics*, *211*, 115–134.

Dold, J. W. (1985), Analysis of the early stage of thermal runaway, *Q. J. Mech. Appl. Math.*, *38*(3), 361–387.

Friedman, A., and Y. Giga (1987), A single point blowup for solutions of semilinear parabolic systems, *J. Fac. Sci. Univ. Tokyo, Sect. 1A*, *34*, 65–79.

Fujita, Ç. (1969), On the non-linear equations $\Delta u + e^u = 0$ and $v_t = \Delta v + e^v$, *Bull. Am. Math. Soc.*, *75*, 132–135.

Galaktionov, V. A., and P. J. Harwin (2005), Non-uniqueness and global similarity solutions for a higher-order semilinear parabolic equation, *Nonlinearity*, *18*, 717–746.

Galaktionov, V. A., and J. Vazquez (1997), Continuation of blowup solutions of nonlinear heat equations in several space dimensions, *Commun. Pure Appl. Math*, *L*, 1–67.

Galaktionov, V. A., and J. Vazquez (2002), The problem of blow up in nonlinear parabolic equations, *Discrete Contin. Dyn. Syst.*, *8*, 399–433.

Garagash, D. I., and J. W. Rudnicki (2003), Shear heating of a fluid-saturated slip-weakening dilatant fault zone 1. Limiting regimes, *J. Geophys. Res.*, *108*(B2), 2121, doi:10.1029/2001JB001653.

Gruntfest, I. J. (1963), Thermal feedback in liquid flow: Plane shear at constant stress, *Trans. Soc. Rheol.*, *7*, 195–207.

Habib, P. (1967), Sur un mode de glissement des massifs rocheaux, *C. R. Seances Acad. Sci.*, *264*, 151–153.

Habib, P. (1975), Production of gaseous pore pressure during rock slides, *Rock Mech.*, *7*, 193–197.

Helmstetter, A., D. Sornette, J.-R. Grasso, J. V. Andersen, S. Gluzman, and V. Pisarenko (2004), Slider block friction model for landslides: Application to Vaiont and La Clapière landslides, *J. Geophys. Res.*, *109*, B02409, doi:10.1029/2002JB002160.

Hendron, A. J. and F. D. Patton (1985), The Vaiont slide, a geotechnical analysis based on new geologic observations of the failure surface, *Tech. Rep. GL-85-5*, U.S. Army Corps of Eng., Washington, D. C.

Hicher, P. Y. (1974), Etude des proprietes mecaniques des argiles a l' aide d' essais triaxiaux, in uence de la vitesse et de la temperature, report, Soil Mech. Lab., Ecole Cent. de Paris, Paris.

Iverson, R. M. (2005), Regulation of landslide motion by dilatancy and pore pressure feedback, *J. Geophys. Res.*, *110*, F02015, doi:10.1029/2004JF000268.

Kaplan, S. (1963), On the growth of solutions of quasilinear parabolic equations, *Commun. Pure Appl. Math.*, *16*, 305–330.

Kilburn, R. J. C., and D. N. Petley (2003), Forecasting giant, catastrophic slope collapse: Lessons from Vajont, northern Italy, *Geomorphology*, *54*, 21–32.

Laloui, L. (2001), Thermo-mechanical behaviour of soils, in *Environmental Geomechanics*, edited by R. Charlier and A. Gens, *Rev. Fr. Genie Civ.*, *5*(6), 809–843.

Laloui, L. (2005), Constitutive modelling of the thermo-plastic behaviour of soils, in *Coupled Multiphysics Processes in Geomechanics*, edited by L. Laloui et al., *Rev. Fr. Genie Civ.*, *9*(5–6), 635–650.

Laloui, L., and C. Cekerevac (2003), Thermo-plasticity of clays: An isotropic yield mechanism, *Comput. Geotech.*, *30*, 649–660.

Leinenkugel, H.-J. (1976), Deformations und Festigkeitverhalten bindiger Erdstoffe: Experimental Ergebnisse und ihre physikalische Deutung, doctoral dissertation, Univ. Karlsruhe, Karlsruhe, Germany.

Leroy, Y. M., and A. Molinari (1992), Stability of steady-states in shear zones, *J. Mech. Phys. Solids*, *40*, 181–212.

Morgenstern, N. R., and J. S. Tschalenko (1967), Microscopic structures in kaolin subjected to direct shear, *Géotechnique*, *17*, 309–328.

Müller, L. (1964), The rock slide in the Vaiont valley, *Felsmech. Ingenieurgeol.*, *2*, 148–212.

Müller-Saltzburg, L. (1968), New considerations on the Vaiont slide, *Felsmech. Ingenieurgeol.*, *6*, 1–91.

Nova, R. (1986), Soil models as a basis for modelling the behaviour of geophysical materials, *Acta Mech.*, *64*, 31–44.

Petley, D. N., F. Mantovani, M. H. Bulmer, and A. Zannoni (2005), The use of surface monitoring data for the interpretation of landslide movement patterns, *Geomorphology*, *66*, 133–147.

Picard, J. (1994), Ecrouisage thermique des argiles saturées: Application au stockage des déchets radioactifs, Thèse de Doctorat, Ecole Natl. des Ponts et Chaussées, Paris.

Planck, M. (1945), *Treatise on Thermodynamics*, p. 44, Dover, Mineola, N. Y.

Rice, J. (2006), Heating and weakening of faults during earthquake slip, *J. Geophys. Res.*, *111*, B05311, doi:10.1029/2005JB004006.

Rosakis, P., A. J. Rosakis, G. Ravichandran, and J. Hodowany (2000), A thermodynamic internal variable model for the partition of plastic work into heat and stored energy in metals, *J. Mech. Phys. Solids*, *48*, 581–607.

Ruina, A. (1983), Slip instability and state variable friction laws, *J. Geophys. Res.*, *88*, 10,359–10,370.

Schochet, S. (1999), Similarity stabilizes blow-up, *J. Equations Derivees Partielles*, *12*, 1–7.
Schwartz, W. (1987), Verdübelung toniger Böden, doctoral dissertation, Univ. Karlsruhe, Karlsruhe, Germany.
Selli, R., and L. Trevisan (1964), Caratteri e interpretazione della frana del Vaiont, *G. Geol.*, *XXXII*, 7–103.
Semenza, E. (1965), Sintesi degli Studi Geologici sulla frana del Vajont dal 1959 al 1964, *Mem. Mus. Tridentino Scie. Nat.*, *XVI*, 1–52.
Sitar, N., M. MacLaughlin, and D. Doolin (2005), Influence of kinematics on landslide mobility and failure mode, *J. Geotech. Geoenviron. Eng.*, *131*(6), 716–728, doi:10.1061/(ASCE)1090-0241(2005)131:6(716).
Sornette, D., A. Helmstetter, J. V. Andersen, S. Gluzman, J. R. Grasso, and V. Pisarenko (2004), Towards landslide predictions: Two case studies, *Physica A*, *338*(3–4), 605–632.
Sulem, J., P. Lazar, and I. Vardoulakis (2007), Thermo-poro-mechanical properties of clayey gouge and application to rapid fault shearing, *Int. J. Numer. Anal. Methods Geomech.*, *31*(3), 523–540.
Sultan, N. (1997), Etude du comportement thermo-méchanique de l' argile de Boom: Expériences et modélisation, Thèse de Doctorat, Cent. d'Enseign. et de Rech. en Mecanique des Sols, Ecole Natl. de Ponts et Chausees, Paris.
Taylor, G. I., and H. Quinney (1931), The plastic distortion of metals, *Philos. Trans. R. Soc. London, Ser., A*, *230*, 323–362.
Tika, T. E., and J. N. Hutchinson (1999), Ring shear tests on soil from the Vaiont landslide slip surface, *Géotechnique*, *49*, 59–74.
Vardoulakis, I. (2000), Catastrophic landslides due to frictional heating of the failure plane, *Mech. Cohesive Frict. Mater.*, *5*, 443–467.
Vardoulakis, I. (2002a), Dynamic thermo-poro-mechanical analysis of catastrophic landslides, *Geotechnique*, *52*, 157–171.
Vardoulakis, I. (2002b), Steady shear and thermal run-away in clayey gouges, *Int. J. Solids Struct.*, *39*, 3831–3844.
Vardoulakis, I. (2002c), Dynamic thermo-poro-mechanical stability analysis of simple sear on frictional materials, in *Modelling and Mechanics of Granular Porous Materials*, edited by G. Capritz, V. N. Ghionna, and P. Giovine, pp. 129–155, Springer, New York.
Voight, B. (1978), *Rockslides and Avalanches*, vol. 1, *Natural Phenomena*, Elsevier, Amsterdam.
Voight, B. (1988), A method for prediction of volcanic eruptions, *Nature*, *332*, 125–130.
Voight, B., and C. Faust (1982), Frictional heat and strength loss in some rapid landslides, *Géotechnique*, *32*, 43–54.
Wibberley, A. J. C., and T. Shimamoto (2005), Earthquake slip weakening and asperities explained by thermal pressurization, *Nature*, *436*, 689–692.
Wood, D. M. (1990), *Soil Behaviour and Critical State Soil Mechanics*, Cambridge Univ. Press, New York.

G. Di Toro, Dipartimento di Geoscienze, Universita' di Padova, Via Giotto 1, 35137 Padua, Italy.
I. Vardoulakis and E. Veveakis, Department of Mechanics, National Technical University of Athens, Theoxaris Bldg., Iroon Politechniou 5, Zografou, 15773 Athens, Greece. (manolis@mechan.ntua.gr)